laser photocoagulation. However, these developments might be visible only angiographically, and clinical changes during the follow-up period, i.e., the pathological and intrinsic changes, were not evident.

Although the study was not population-based, we reported that the proportion of PCV is more than 50% in Japanese patients with neovascular AMD, and that PCV and typical AMD are male predominant, unilateral, and without large drusen in the fellow eye [13]. Thus, both PCV and typical AMD have similar demographic features and might be the same disease group with different clinical expressions. It is interesting that in some combined cases, one eye had PCV and the other eye had typical AMD under the same systemic conditions in the current study.

The Hisayama study reported that the prevalence of drusen was 9.8% in Japanese people [17]. This is a very small percentage compared to reports from Western countries. Although Japanese patients do not have much drusen, basal laminar deposits, which are recognized as a lesion of age-related maculopathy, were observed in elderly Japanese patients and Caucasian patients [6]. In addition, one of the major and important neovascular AMD genes, the *HtrA serine peptidase 1* (*HTRA1*) gene at location 10q26, has been identified in both Caucasian and Chinese patients [3, 21]. *HTRA1* also has been reported equally in Japanese patients with AMD [16, 22]. Some researchers have reported that the LOC387715/HTRA1 variants or ARMS2 (age-related maculopathy susceptibility 2)/HTRA1 variants were associated with PCV and typical AMD in a Japanese population, which suggested that PCV and typical AMD are similar in genetic susceptibility [4, 5, 11]. Although a large number of patient studies are needed, the elastin gene haplotype was reported to be associated with the different phenotypes of PCV and typical AMD [10]. Ladas and associates [12] reported that polypoidal lesions developed in patients with Doyne's familial honeycomb choroiditis, which is usually thought to occur with inherited, drusen-related, secondary CNV instead of PCV. This might indicate that the development to either PCV or typical AMD is not based on genetic factors only.

The eyes with PCV had a lower mean BCVA and a larger mean lesion area than the eyes with typical AMD at the initial examination. Most PCV cases had a better prognosis; however, some cases with recurrent bleeding and exudation had a poor prognosis. In the combined cases in the current study, the eyes with PCV seemed to have an unfavorable prognosis. Meanwhile, the eyes with typical AMD might have had a favorable prognosis. However, the eyes that developed to polypoidal lesions had a lower BCVA and a larger lesion area than the eyes that did not develop polypoidal lesion in the eyes with typical AMD. These differences in the mean BCVA and lesion area might depend on the duration of the disorder in the combined cases.

The diagnostic criteria for PCV have not yet been established in the presumed PCV cases without polypoidal lesions. In the Japanese Study Group of Polypoidal Choroidal Vasculopathy [7], probable cases of PCV were defined by the presence of at least one of the following: only an abnormal vascular network seen on ICGA and recurrent hemorrhagic and/or RPE serous detachments. In the current study, half of the eyes with typical AMD diagnosed at the initial examination had a polypoidal lesion on ICGA during the follow-up period (range, 2–48 months). Some eyes with typical AMD might be diagnosed as probable cases based on the Japanese Study Group of Polypoidal Choroidal Vasculopathy [7]. Only patients with an abnormal vascular network of PCV without a polypoidal lesion on ICGA might be considered as having occult CNV associated with typical AMD, because the abnormal vascular network of PCV often shows leakage on FA or ICGA. Thus, it is difficult even for retina specialists to distinguish the abnormal vascular network without a polypoidal lesion from CNV under the RPE (e.g., type 1 CNV). Further study is needed to accurately diagnose the probable cases of PCV in a clinical setting.

In conclusion, we observed combined cases in which one eye had PCV and the other eye had typical AMD in patients with neovascular AMD. Although some cases might include those with different stages or probable cases of PCV, the combined cases in the current study might imply that both clinical entities are not independent and possibly overlap.

Funding None.

Competing interests None.

References

1. Ali F, Chan WC, Stevenson MR, Muldrew KA, Chakravarthy U (2004) Morphometric analysis of angiograms of exudative lesions in age-related macular degeneration. Arch Ophthalmol 122:710–715. doi:10.1001/archopht.122.5.710
2. Barbazetto I, Burdan A, Bressler NM, Bressler SB, Haynes L, Kapetanios AD, Lukas J, Olsen K, Potter M, Reaves A, Rosenfeld P, Schachat AP, Strong HA, Wenkstern A, Treatment of Age-Related Macular Degeneration with Photodynamic Therapy Study Group (2003) Verteporfin in Photodynamic Therapy Study Group. Photodynamic therapy of subfoveal choroidal neovascularization with verteporfin: fluorescein angiographic guidelines for evaluation and treatment–TAP and VIP report No. 2. Arch Ophthalmol 121:1253–1268. doi:10.1001/archopht.121.9.1253
3. Dewan A, Liu M, Hartman S, Zhang SS, Liu DT, Zhao C, Tam PO, Chan WM, Lam DS, Snyder M, Barnstable C, Pang CP, Hoh J (2006) HTRA1 promoter polymorphism in wet age-related macular degeneration. Science 314:989–992. doi:10.1126/science.1133807

4. Gotoh N, Nakanishi H, Hayashi H, Yamada R, Otani A, Tsujikawa A, Yamashiro K, Tamura H, Saito M, Saito K, Iida T, Matsuda F, Yoshimura N (2009) ARMS2 (LOC387715) Variants in Japanese Patients with Exudative Age-related Macular Degeneration and Polypoidal Choroidal Vasculopathy. Am J Ophthalmol 147:1037–1041. doi:10.1016/j.ajo.2008.12.036
5. Gotoh N, Yamada R, Nakanishi H, Saito M, Iida T, Matsuda F, Yoshimura N (2008) Correlation between CFH Y402H and HTRA1 rs11200638 genotype to typical exudative age-related macular degeneration and polypoidal choroidal vasculopathy phenotype in the Japanese population. Clin Exper Ophthalmol 36:437–442. doi:10.1111/j.1442-9071.2008.01791.x
6. Ishibashi T, Patterson R, Ohnishi Y, Inomata H, Ryan SJ (1986) Formation of drusen in the human eye. Am J Ophthalmol 101:342–353
7. Japanese Study Group of Polypoidal Choroidal Vasculopathy (2005) Criteria for diagnosis of polypoidal choroidal vasculopathy (in Japanese). Nippon Ganka Gakkai Zasshi 109:417–427
8. Klein R, Klein BE, Jensen SC, Meuer SM (1997) The five-year incidence and progression of age-related maculopathy: the Beaver Dam Eye Study. Ophthalmology 104:7–21
9. Klein R, Klein BE, Tomany SC, Meuer SM, Huang GH (2002) Ten-year incidence and progression of age-related maculopathy: The Beaver Dam Eye Study. Ophthalmology 109:1767–1779. doi:10.1016/S0161-6420(02)01146-6
10. Kondo N, Honda S, Ishibashi K, Tsukahara Y, Negi A (2007) LOC387715/HTRA1 variants in polypoidal choroidal vasculopathy and age-related macular degeneration in a Japanese population. Am J Ophthalmol 144:608–612. doi:10.1016/j.ajo.2007.06.003
11. Kondo N, Honda S, Ishibashi K, Tsukahara Y, Negi A (2008) Elastin gene polymorphisms in neovascular age-related macular degeneration and polypoidal choroidal vasculopathy. Invest Ophthalmol Vis Sci 49:1101–1105. doi:10.1167/iovs.07-1145
12. Ladas ID, Karagiannis DA, Georgalas I, Rouvas AA, Moschos MM, Apostolopoulos M (2004) Polypoidal choroidal vasculopathy associated with Doyne's familial choroiditis: treatment with thermal laser. Eur J Ophthalmol 14:264–268
13. Maruko I, Iida T, Saito M, Nagayama D, Saito K (2007) Clinical characteristics of exudative age-related macular degeneration in Japanese patients. Am J Ophthalmol 144:15–22. doi:10.1016/j.ajo.2007.03.047
14. Mitchell P, Wang JJ, Foran S, Smith W (2002) Five-year incidence of age-related maculopathy lesions: the Blue Mountains Eye Study. Ophthalmology 109:1092–1097. Erratum in: Ophthalmology (2002) 109:1588. doi:10.1016/S0161-6420(02)01055-2
15. Miyazaki M, Kiyohara Y, Yoshida A, Iida M, Nose Y, Ishibashi T (2005) The 5-year incidence and risk factors for age-related maculopathy in a general Japanese population: the Hisayama study. Invest Ophthalmol Vis Sci 46:1907–1910. doi:10.1167/iovs.04-0923
16. Mori K, Horie-Inoue K, Kohda M, Kawasaki I, Gehlbach PL, Awata T, Yoneya S, Okazaki Y, Inoue S (2007) Association of the HTRA1 gene variant with age-related macular degeneration in the Japanese population. J Hum Genet 52:636–641. doi:10.1007/s10038-007-0162-1
17. Oshima Y, Ishibashi T, Murata T, Tahara Y, Kiyohara Y, Kubota T (2001) Prevalence of age related maculopathy in a representative Japanese population: the Hisayama study. Br J Ophthalmol 85:1153–1157. doi:10.1136/bjo.85.10.1153
18. Treatment of Age-related Macular Degeneration With Photodynamic Therapy (TAP) Study Group (1999) Photodynamic therapy of subfoveal choroidal neovascularization in age-related macular degeneration with verteporfin: one-year results of 2 randomized clinical trials–TAP report. Arch Ophthalmol 117:1329–1345
19. Uyama M, Wada M, Nagai Y, Matsubara T, Matsunaga H, Fukushima I, Takahashi K, Matsumura M (2002) Polypoidal choroidal vasculopathy: natural history. Am J Ophthalmol 133:639–648. doi:10.1016/S0002-9394(02)01404-6
20. Vingerling JR, Dielemans I, Hofman A, Grobbee DE, Hijmering M, Kramer CF, de Jong PT (1995) The prevalence of age-related maculopathy in the Rotterdam Study. Ophthalmology 102:205–210
21. Yang Z, Camp NJ, Sun H, Tong Z, Gibbs D, Cameron DJ, Chen H, Zhao Y, Pearson E, Li X, Chien J, Dewan A, Harmon J, Bernstein PS, Shridhar V, Zabriskie NA, Hoh J, Howes K, Zhang K (2006) A variant of the HTRA1 gene increases susceptibility to age-related macular degeneration. Science 314:992–993. doi:10.1126/science.1133811
22. Yoshida T, DeWan A, Zhang H, Sakamoto R, Okamoto H, Minami M, Obazawa M, Mizota A, Tanaka M, Saito Y, Takagi I, Hoh J, Iwata T (2007) HTRA1 promoter polymorphism predisposes Japanese to age-related macular degeneration. Mol Vis 13:545–548

Infrared Fundus Autofluorescence and Central Serous Chorioretinopathy

Tetsuju Sekiryu, Tomohiro Iida, Ichiro Maruko, Kuniharu Saito, and Takeshi Kondo

Purpose. To investigate the findings of infrared fundus autofluorescence in eyes with central serous chorioretinopathy (CSC).

Methods. This study was an observational follow-up of 83 eyes of 80 consecutive patients with CSC recruited from a hospital referral practice. Infrared autofluorescence (IR-AF) findings and those of other clinical studies, including short-wave autofluorescence (SW-AF), fundus color photography, and optical coherence tomography were assessed. The IR-AF changes that appeared during the follow-up period were recorded. The relationship between IR- and SW-AF was analyzed by comparing the categories of focal autofluorescence (granular hyper-AF, granular hypo-AF, and mixed AF). The influence of final clinical findings on final best corrected visual acuity (BCVA) was analyzed.

Results. Twenty-three of 83 (27%) eyes showed granular hyper-IR-AF, whereas 53 (64%) eyes showed granular hyper-SW-AF. Most of the eyes with granular hyper-IR-AF (92%) showed granular hyper-SW-AF. On the contrary, the eyes with granular hyper-SW-AF showed various patterns of IR-AF. The deposits with hyper-IR-AF corresponding to hyper-SW-AF turned into hypo-IR-AF with hyper-SW-AF in four eyes. Final BCVA was significantly worse in eyes with granular hypo-IR-AF compared with the eyes without the findings ($P = 0.035$).

Conclusions. Granular hyper-IR-AF from the deposits in CSC appeared concurrently with hyper-SW-AF. Granular hyper-IR-AF changed from hyperautofluorescence to hypoautofluorescence during the follow-up period. This change of IR-AF characteristics was different from that of SW-AF. The changes are attributable to the modification of melanin in the RPE. The authors speculate that the lipofuscin-like materials contribute to the characteristic changes of IR-AF through the modification of melanin in the RPE. (*Invest Ophthalmol Vis Sci.* 2010;51: 4956–4962) DOI:10.1167/iovs.09-5009

Central serous chorioretinopathy (CSC) is characterized by serous retinal detachment (SRD) at the macula with a focal area or multifocal areas of leakage at the level of the retinal pigment epithelium (RPE) noted on fluorescein angiography (FA). Most patients with acute CSC have spontaneous resolution of their macular detachments and a good visual prognosis. The eyes with long-standing SRD show widespread alteration of the RPE with a decline in visual acuity.[1–4] Imaging technology has provided important information about the disease. Indocyanine green angiography (IA) has indicated dysfunction of the hemodynamics and fluid dynamics in the choroid.[5–7] Optical coherence tomography (OCT) has demonstrated morphologic changes in eyes with CSC, such as swelling of the sensory retina, disruption of the RPE, thickening of the outer retinal surface, and loss of the boundary of the photoreceptor inner/outer segments.[8–10]

Fundus autofluorescence (AF) imaging is a novel imaging technology that can show characteristics of eyes with CSC. A recent report has suggested that fundus AF can predict visual acuity in eyes with CSC.[11] Fundus AF mainly originates from lipofuscin in the RPE, which is a residue of phagocytized photoreceptor outer segments.[12] A major fluorophore of lipofuscin is pyridinium bisretinoid (A2E), which is derived from retinol.[13–15] A recent study suggested that the precursors of A2E in the sensory retina also showed AF and had cytotoxic effects.[16] Dot-like deposits located in the sensory retina or subretinal space show hyper-AF and may be involved in the pathologic changes in CSC.[11,17,18] However, the process causing the degenerative changes in the retina and the RPE remain unclear.

Melanin in the RPE plays an important role in the protection of eyes against phototoxicity that may be involved in age-related dysfunction of the fovea.[19] So far, we do not have a method of evaluating melanin in living eyes. High-definition imaging systems, such as the confocal scanning laser ophthalmoscope, make it possible to visualize faint infrared autofluorescence (IR-AF). Fundus IR-AF can originate from melanin in the RPE or choroidal tissue.[20,21] Imaging of IR-AF may provide new information on the pathologic process in eyes with CSC. We assessed the characteristics of IR-AF in comparison with short-wave autofluorescence (SW-AF), color fundus images, and OCT findings. The present study especially focused on focal IR-AF of subretinal deposits.

Methods

Eighty consecutive patients were examined and CSC with SRD involving the fovea was diagnosed and then confirmed by OCT and FA at Fukushima Medical University Hospital, Fukushima, Japan, between July 2006 and October 2008. Sixty-one (73.4%) men and 19 (26.6%) women were observed longitudinally for 3 to 32 months (mean, 11.8). Three patients were affected with CSC in both eyes. As a result, we studied 83 eyes of 80 patients. After informed consent, each patient was initially examined by visual acuity testing, ophthalmoscopy, color and red-free monochromatic photography, FA, IA, OCT imaging, and fundus AF. The tenets of the Declaration of Helsinki were observed. The Institutional Review Board of the University of Fukushima Medical School granted approval for this study design. Eyes were excluded if they had undergone laser photocoagulation and had melanotic lesions in the fundus and if additional disease was present that could compromise visual acuity.

Fundus Imaging

Visual acuity testing, fundus photography, fundus AF, and OCT images were taken at all visits. Fundus photography was performed with a

From the Department of Ophthalmology, Fukushima Medical University School of Medicine, Fukushima, Japan.

Submitted for publication December 1, 2009; revised March 17, 2010; accepted April 1, 2010.

Disclosure: **T. Sekiryu**, None; **T. Iida**, None; **I. Maruko**, None; **K. Saito**, None; **T. Kondo**, None

Corresponding author: Tetsuju Sekiryu, 960-1295, 1 Hikarigaoka, Fukushima City, Fukushima Pref., Japan; sekiryu@fmu.ac.jp.

Investigative Ophthalmology & Visual Science, October 2010, Vol. 51, No. 10

fundus camera (TRC-50IX; Topcon, Tokyo, Japan). SW- and IR-AF were recorded with a confocal scanning laser ophthalmoscope (HRA2; Heidelberg Engineering, Heidelberg, Germany). The pairs of excitation laser and detection filters were 488 and >500 nm in SW-AF and 787 and >800 nm in IR-AF, respectively. The field was 30° × 30° (768 × 768 pixels). AF images were taken after maximum pupillary dilation with 0.5% tropicamide and 0.5% phenylephrine. Focusing was achieved at 815 nm, and reflectance images were taken. After a switch to the 787-nm excitation (indocyanine green mode), the sensitivity was increased until the vessels and the disc were recognized. Sixteen serial images were processed instantly by the averaging method of the system software (HRA2; Heidelberg Engineering) to gain contrast of the images. SW-AF images (excitation, 488 nm) were acquired in the same manner as the IR-AF images. SW images were taken after sufficient light exposure, because the intensity of SW-AF is changed by light exposure.[22] Images taken within 1 month after IA were eliminated from the analysis to avoid misreading due to residual fluorescence.

OCT scans (OCT-3000-TM, Carl Zeiss Meditec, Jena, Germany; 3D-OCT-TM system Topcon, Tokyo, Japan; Spectralis-TM, Heidelberg Engineering, Heidelberg, Germany) with single scans in the horizontal and vertical orientations were made through the center of the fovea, routinely. OCT-3000-TM was used until July 2007, 3D-OCT-TM was used from August 2007 to March 2008, and Spectralis-TM was used after February 2008. Multihorizontal scans were performed through extrafoveal areas of subretinal fluid in the posterior pole as well. All sets of images obtained during the visits of all patients were analyzed.

Image Analysis

The AF classification and the clinical findings are shown in Table 1. We evaluated three types of AF: background AF, focal AF, and atrophic lesion AF. Background AF was classified into two categories: reduced AF (Figs. 1A, 1B) and diffuse hyper-AF in the area affected by to the SRD (Figs. 1D, 1G, 1H). Focal AF was classified into three categories: granular hyper-AF (Figs. 1G, 1H, 1J), granular hypo-AF (Fig. 1N), and mixed AF (Fig. 2). Herein, focal AF was spotty AF corresponding to deposits or precipitates; granular hyper-AF was composed of dot-like (<63 μm) or fleck-like (63 or >63 μm) hyper-AF exclusively; and granular hypo-AF described the lesions composed of dot- or fleck-like hypo-AF exclusively. Autofluorescence associated with atrophic lesions showed extensive diffuse hypo-AF with unclear boundaries (Fig. 3).

In color fundus photographs, the deposits and fibrin were evaluated. Deposits included both yellow precipitates (<63 μm) and flecks (63 or >63 μm). The OCT findings were classified into four categories: SRD, deposit on the outer retinal surface, deposit on the RPE, and pigment epithelial detachment (PED).

The findings from all image sets of 83 eyes were entered on a computer spreadsheet. Each image was evaluated by two independent graders, with discrepancies resolved by open adjudication with the third grader. The incidence of each finding was calculated for the 83 eyes. The relationships between IR- and SW-AF were analyzed by comparing the characteristics of focal AF.

TABLE 1. Classification of the Findings

A. Classification of Autofluorescence*

	Type of AF	Categories
IR-AF and SW-AF	Background AF	Reduced AF
		Diffuse hyper-AF
	Focal AF	Granular hyper-AF
		Granular hypo-AF
		Mixed AF
	AF associated with atrophy	Diffuse hypo-AF

B. Classification of Color Fundus Photographs and OCT†

	Findings
Fundus photograph	Deposits
	Fibrin
OCT	SRD
	PED
	Deposits on the outer retina
	Deposits on the RPE

* Fundus autofluorescence (AF) was classified into three categories: background AF, focal AF, and AF associated with atrophy. Background AF corresponded to the whole area affected by SRD. Focal AF was spotty and corresponded to deposits or precipitates. Granular hyper-AF was composed of dot-like (<63 μm) or fleck-like (63 or >63 μm) hyper-AF exclusively. Granular hypo-AF was composed of dot-like and fleck-like hypo-AF exclusively. Mixed AF was both hyper- and hypo-AF appearing within the affected area.

† In color fundus photograph, deposits included both yellow precipitates and flecks.

Final Visual Acuity

To evaluate the relationships between the findings listed (Table 1) and the final best corrected visual acuity (BCVA), final BCVA in the eyes with the clinical findings was compared with that in the eyes without findings by univariate analysis.

Statistical Methods

Logarithm of the minimum angle of resolution (logMAR) was used for statistical analysis and was converted to decimal acuity equivalents. The data obtained were analyzed with frequency and descriptive statistics. The final BCVA was compared between the group with the clinical findings and without findings by using the Mann-Whitney U test. $P < 0.05$ was considered significant in the statistical analyses (JMP 7.0; SAS, Cary, NC).

Results

The mean age of the patients was 48.9 years (SD, 8.9; range 25–65). No patient had choroidal neovascularization. The mean of the final BCVA was 0.92 (range, 0.15–2.0). One hundred four leakage points were identified by FA in the 83 eyes. The eyes with two or more leaking points were included. The type of the leakage points in FA included inkblot 84.3% (70/83 eyes), smokestack 15.6% (13/83 eyes), and diffuse leakage 9.6% (10/83 eyes). In IR-AF images, leakage points showed hypo-AF 83.7% (87/104 leakage points), hyper-AF 3.8% (4/104 leakage points), and iso-AF 12.4% (13/104 leakage points), respectively. Fourteen eyes showed a recurrence after complete resolution of SRD, which was confirmed by OCT. Forty-seven of the 83 eyes were observed for more than 6 months.

AF Findings

A summary of the clinical findings that appeared throughout the follow-up period is shown in Figure 4. For background AF, reduced IR-AF appeared in 31 (37%) eyes in the acute stages of CSC, and diffuse hyper-IR-AF appeared in 69 (83%) eyes. Reduced IR-AF turned into diffuse hyper-IR-AF in 20 (64%) of 31 eyes during the follow-up period. The incidence of the focal IR-AF findings in 83 eyes was as follows; granular hyper-IR-AF, 23 (28%); granular hypo-IR-AF, 21 (25%), and mixed IR-AF, 19 (23%) (Fig. 4). To assess the interobserver variability in background AF and focal AF, κ statistics were calculated. The interobserver variability was 0.78 (background IR-AF), 0.75 (background SW-AF), 0.83 (focal IR-AF), and 0.84 (focal SW-AF).

Twenty-one of 23 eyes with granular hyper-IR-AF appeared concurrently with diffuse hyper-IR-AF, whereas the remainder of two eyes appeared with reduced IR-AF. Granular hyper-AF

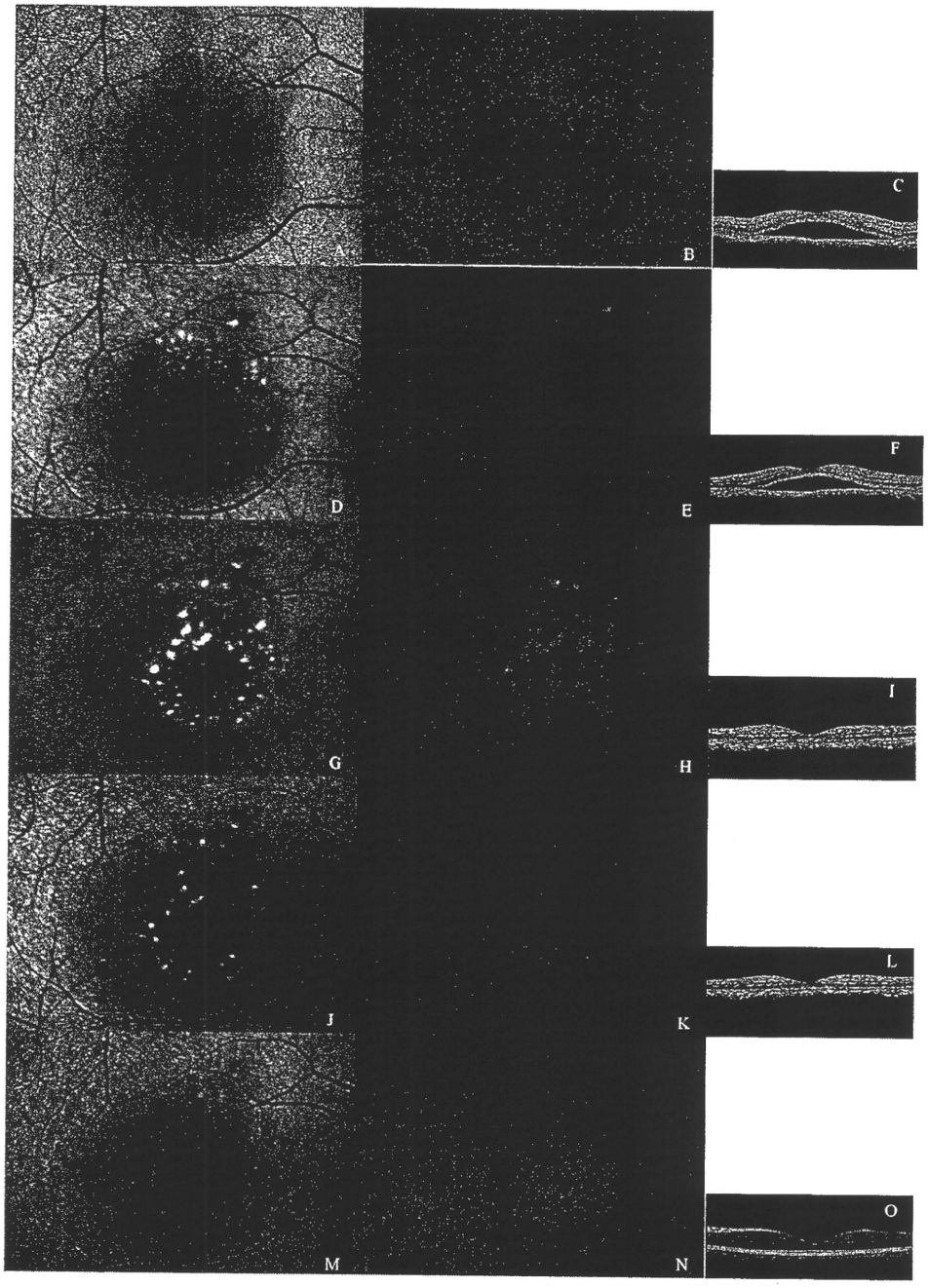

FIGURE 1. AF and OCT images of patient 1, a 34-year-old man. Images of SW-AF (**A**, **D**, **G**, **J**, **M**), IR-AF (**B**, **E**, **H**, **K**, **N**), and OCT (**C**, **F**, **I**, **L**, **O**) in the right eye. (**A–C**) Two weeks after onset, the area with SRD showed hypo-SW-AF and hypo-IR-AF. OCT showed no deposits on the outer retinal surface and the RPE. (**D–F**) Six weeks after onset, SW-AF showed multiple dot-like hyper-AF (**D**). IR-AF showed no dot-like hyper-AF except around the leak. OCT demonstrated deposits on the outer retinal surface at the center of the fovea. (**G–I**) Ten weeks after onset, SRD had resolved spontaneously (**I**). Flecks with hyper-AF appeared in both the images of SW- and IR-AF (**G**, **H**). (**J–L**) Eight weeks after reattachment, flecks of hyper-SW-AF and hyper-IR-AF had decreased in number and size. IR-AF showed diffuse hyper-AF in the affected area (**J**, **K**). (**M–O**) Eighteen months after reattachment, flecks with hyper-SW-AF showed hypo-IR-AF (**M**, **N**).

appeared more frequently in SW-AF imaging compared with IR-AF imaging, whereas granular hypo-AF was observed less frequently in SW-AF imaging. Two eyes with mass deposits that showed homogenous hyper-SW-AF were classified as mixed SW-AF (see Fig. 7). In color fundus photographs, 83% (72/83) of the eyes showed deposits. In OCT images, the deposit appeared on the outer retinal surface in 56 (67%) eyes and on the RPE in 54 (65%). PED away from the leakage point was noted in 19 (23%) eyes.

Focal AF findings included four categories: no focal AF, granular hyper-AF, granular hypo-AF, and mixed AF. Therefore, the combinations of focal IR- and SW-AF findings include 16 pairs of AF findings. To analyze the relationships between IR- and SW-AF, we evaluated the appearance of 16 pairs of AF categories during the follow-up period (see Fig. 8). A total of 117 paired AF findings were observed in 83 eyes throughout the follow-up period. Twenty-two (92%) of 24 eyes with granular hyper-IR-AF showed granular hyper SW-AF. The eyes with granular hyper-IR-AF showed neither granular hypo- nor mixed SW-AF. On the contrary, 64 eyes with granular hyper-SW-AF showed hypo (8 eyes/13%) or mixed IR-AF (12 eyes/19%). Dot-like hyper-SW-AF showed iso- or hypo- IR-AF in the acute stages of CSC (Figs. 1, 5). Fleck-like deposits with hyper-SW-AF and hypo-IR-AF appeared after resolution of SRD (Fig. 1). Granular hyper-IR-AF turned into granular hypo-IR-AF in 4 of 24 eyes during the follow-up period. In OCT images, some deposits with hyper-IR-AF corresponded to the mound of RPE (Fig. 6).

Final BCVA

The difference in final BCVA between the group with and the one without clinical findings was examined in 47 eyes that were observed for more than 6 months. Analyzed categories are follows: reduced-IR-AF, diffuse hyper-IR-AF, granular hyper-

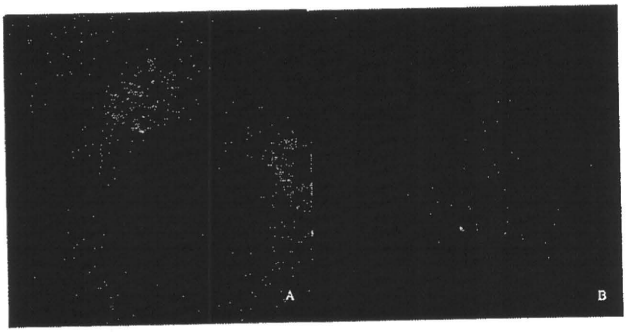

FIGURE 2. AF images classified as mixed-AF. SW-AF image (**A**) shows granular hypo-AF among granular hyper-AF. Granular hypo-AF was more prominent in the IR-AF images (**B**). They were classified as mixed-AF.

IR-AF, granular hypo-IR-AF, mixed IR-AF, diffuse hypo-IR-AF, reduced-SW-AF, diffuse hyper-SW-AF, granular hyper-SW-AF, granular hypo-SW-AF, mixed SW-AF, diffuse hypo-SW-AF, deposits, fibrin, SRD, PED, deposits on the outer retina, and deposits on the RPE. Final BCVA decreased significantly in the eyes showing granular hypo-IR-AF ($P = 0.035$) by the Mann-Whitney test. BCVAs of the eyes with deposits on fundus photograph and PED in OCT were worse than in eyes without the findings; however, the difference was not statistically significant (deposit; $P = 0.09$, PED; $P = 0.09$).

DISCUSSION

We compared the findings of IR-AF with SW-AF and other clinical findings, to study the characteristics of IR-AF in the eyes with CSC. Characteristics of IR-AF changed during the course of CSC. Background AF within SRD showed hypo-IR-AF and hypo-SW-AF in the acute stage, which then turned into diffuse hyper-AF during the follow-up period in both SW-AF and IR-AF images. In focal AF, although the dot-like deposits in SRD showed hyper-AF in SW-AF imaging, they showed iso- or hypo-AF in IR-AF imaging. Fleck-like deposits with hyper-SW-AF concurrently showed hyper-IR-AF, just after resolution of SRD. IR-AF of these deposits turned into hypo-IR-AF after more than a year.

Lipofuscin in the RPE is an assortment of major chromophores derived from photoreceptor breakdown and accumulates in the RPE throughout life. A2E and its precursors, which are the main components of lipofuscin, show SW-AF and provide functional information on the RPE. Melanin is an insoluble high-molecular-weight polymer derived from the enzymatic oxidation of tyrosine and dihydroxyphenylalanine.[23] Melanin in the RPE plays an important role in the protection of eyes against phototoxicity. The protective effects of melanin

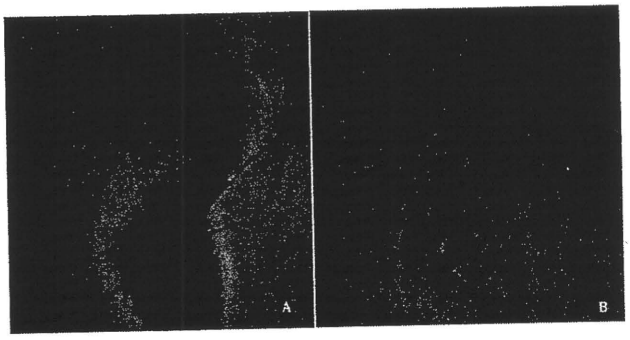

FIGURE 3. AF images show diffuse hypo-AF. (**A**) SW-AF image. (**B**) IR-AF image.

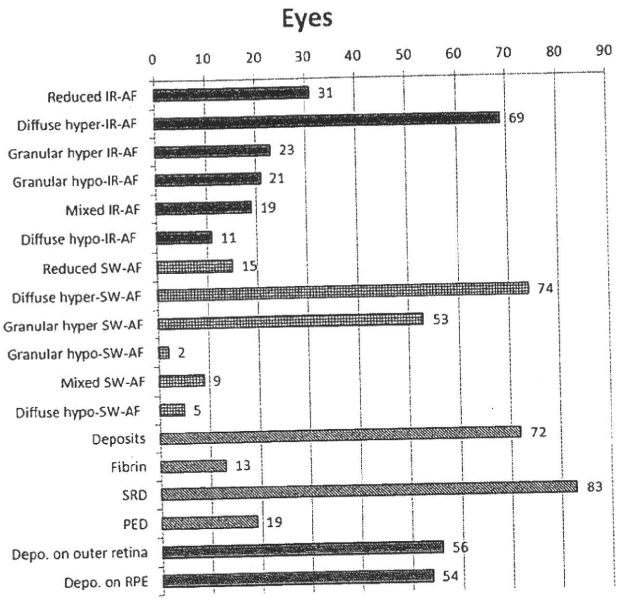

FIGURE 4. Summary of findings. The numbers represent the number of eyes affect of the 83 examined. Depo, deposit.

are ascribed to its antioxidant property and photo-screening effects.[24–26] It is presumed that the reduction of its protective effects, due to diminished melanin with age, is the pathogenesis of age-related macular degeneration.[19] So far, we do not have a method of evaluating melanin in living eyes. Recent reports suggested that IR-AF was generated from the melanin in the RPE and the choroid.[20,21] The combination of IR- and SW-AF imaging is potentially a useful tool for assessing the functional aspects of the RPE. To explain the interpretation of IR-AF in CSC, we studied the IR-AF findings and their relation to the other clinical findings.

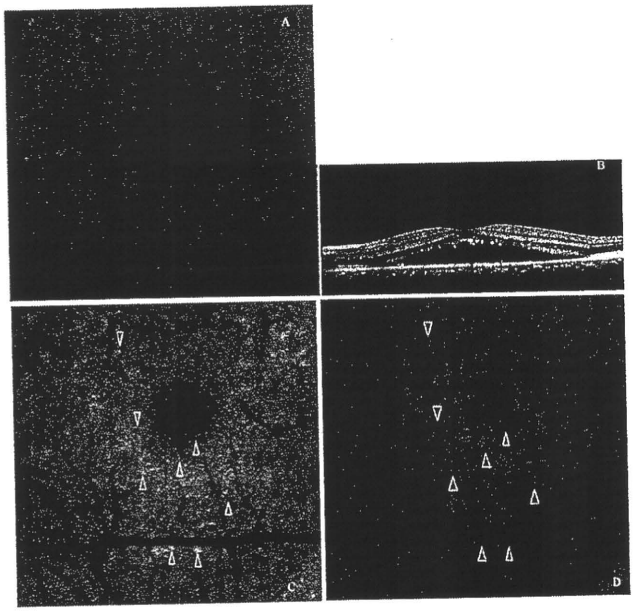

FIGURE 5. AF and OCT images of the right eye of patient 2, a 38-year-old man. (**A**) Red-free photograph. Precipitate appeared within the area of SRD. (**B**) Vertical OCT image shows dot-like deposits on the outer retinal surface. (**C**) An SW-AF image showing hyper-SW-AF within the area of SRD. (**D**) An IR-AF image showing dot-like hyper-SW-AF corresponding to dot-like hypo-IR-AF (*arrowheads*).

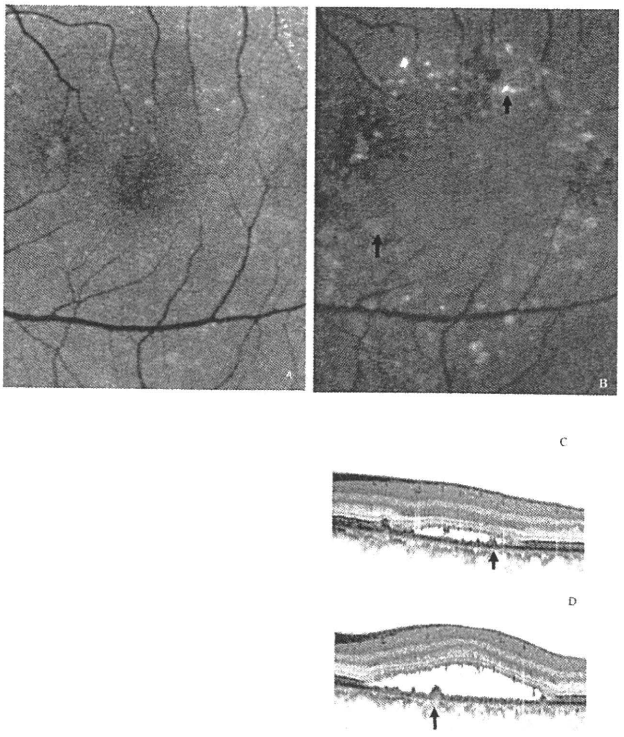

FIGURE 6. AF and OCT images of the left eye of patient 3, a 56-year-old man. The retina was detached 6 months after onset of SRD. SW-AF (**A**) and IR-AF (**B**) at high magnification and pairs of IR-AF images and spectral domain OCT (**C**, **D**). The affected area showed diffuse hyper-SW-AF and hyper-IR-AF. Dot-like hyper-IR-AF was not observed at the fovea (**B**). Some fleck-like hyper-IR-AF corresponded to hyper-SW-AF. Some flecks of hyper-IR-AF corresponded to the mound of the RPE (*arrows*) (**C**, **D**).

AF Characteristics of Deposits

Subretinal deposits are considered to be accumulations of photoreceptor outer segments or phagocytized outer segments by macrophages. They may contribute to retinal degeneration in eyes with CSC.[11] In attempting to evaluate the characteristics of the deposits by using IR-AF, one obstacle is the diversity of IR-AF. For example, one of the fleck-like hyper-SW-AF images shows hyper-IR-AF and another fleck-like hyper-SW-AF image shows hypo-IR-AF. The diversity of IR-AF can be attributed to the masking effect of fibrin or lipid in the subretinal space. In addition, the difference in sensitivity between IR- and SW-AF using the HRA2 system may modify the IR-AF findings.

To reduce modification factors, the focal AF was classified into three categories from the appearance of focal AF within the affected area. Dot-like hyper-SW-AF in SRD without fibrin or lipids, showed iso- or hypo-IR-AF. In addition, flecks with hyper-SW-AF showed hypo-IR-AF after reattachment of the retina (Figs. 1, 7). These results suggested that the subretinal deposits exhibit different characteristics of AF in IR-AF imaging from SW-AF imaging, regardless of modification factors.

Causes of Hyper-IR-AF

The eyes with granular hyper-IR-AF showed granular hyper-SW-AF concurrently in the course of CSC, but not vice versa. In most deposits, hyper-IR-AF colocalized with hyper-SW-AF (Fig. 8). Aggregation of the RPE can show hyper-IR-AF.[27] Since the RPE contains melanin and lipofuscin, the masses of

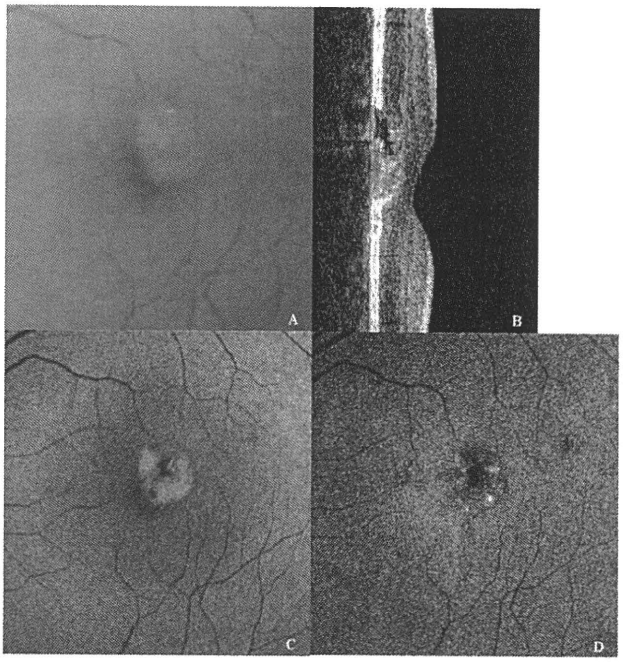

FIGURE 7. AF and OCT images of patient 4 shows a mass of hyper-SW-AF in a color fundus photograph. (**A**) *Yellow* deposit accumulated in the inferior half of SRD. (**B**) Vertical OCT image demonstrated that the deposit occupied more than half of the SRD. (**C**) Three quarters of the affected area showed hyper-SW-AF. (**D**) An IR-AF image did not show hyper-AF corresponding to hyper-SW-AF. Hyper-AF spots appeared at the edge of the *yellow* deposit.

RPE cells can generate both SW- and IR- hyper-AF. High-resolution OCT revealed that the hyper-IR-AF appearance corresponded to the focal mound of the RPE (Fig. 6). However, aggregation of the RPE could not explain all the kinds of hyper-IR-AF, especially the diffuse hyper-IR-AF in the area without protrusion of the RPE on the OCT images (Fig. 1H). Yellow dot-like deposits in the acute stage of CSC or the yellow mass of the deposits are considered to contain lipofuscin-like materials. Since they did not show hyper-IR-AF, hyper-IR-AF may originate from melanin and not from lipo-

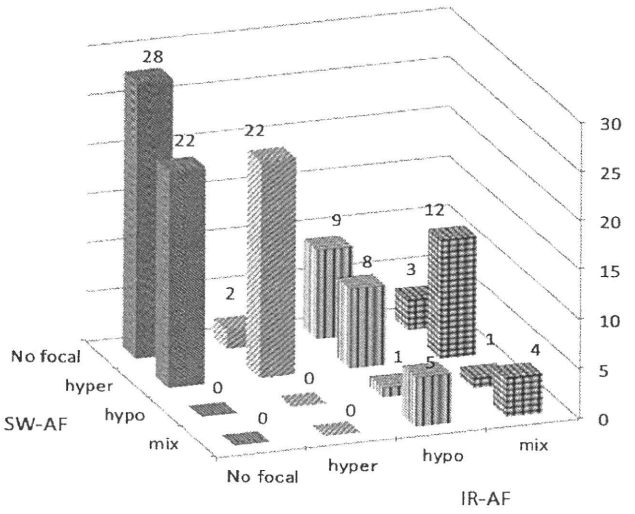

FIGURE 8. The relationships of focal AF. One hundred seventy-nine paired AF findings appeared during the follow-up period in 116 eyes. No focal, eye with no focal AF; Hyper, eye with granular hyper-AF; Hypo, eye with granular hypo-AF; Mixed, eye with mixed AF.

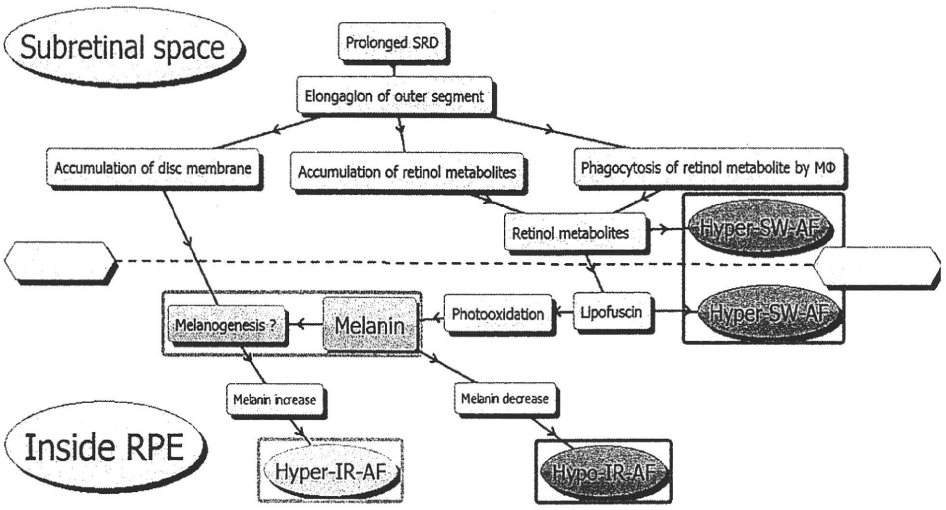

FIGURE 9. A model of IR-AF and related events. Prolonged SRD causes the elongation of the outer segments of photoreceptors. Degraded disc membrane and retinol metabolites are stored in the elongated outer segments. Retinol metabolites acquire SW-AF, especially after they are phagocytized by macrophages or microglia. After the loss of the outer segment or reattachment, the degraded outer segment is processed in the RPE. The disc membrane can induce melanogenesis, causing hyper-IR-AF. Pigmentation increases as a result of melanogenesis. A large amount of residual lipofuscin in the RPE induces photo-oxidation of melanin, which reduces the amount of melanin. As a result, flecks with hyper-SW-AF show hypo-IR-AF.

fuscin-like materials, during CSC (Fig. 7). Melanogenesis in the RPE may be possible, and experimental reports suggest that melanogenesis is induced by feeding of the outer segments of photoreceptor.[28–31] This melanogenesis was presumed to occur by using the disc membrane of outer segments as a substrate. OCT revealed the elongation of outer segments of photoreceptor in the eyes with CSC.[32] Reattachment of the retina may give similar circumstances to the outer segment feeding model. However, postnatal melanogenesis in the RPE cells is controversial.[33–35] A final possibility is that the changes in the IR-AF property by photoactivation may be involved in hyper-IR-AF.[36] At this point, increases in IR-AF induced by melanogenesis and photooxidation have not been shown in the living human eye. A further experimental study is needed to address this point.

Causes of Hypo-IR-AF

SRD and PED showed hypo-IR-AF, caused by the attenuation of IR-AF from the RPE or the choroid by the accumulated fluid. The other types of hypo-IR-AF were shown in focal IR-AF. Hypo-IR-AF with hypo-SW-AF is thought to be due to the loss of RPE or a strong masking effect such as could be caused by debris or components of blood. However, hypo-IR-AF appeared on the deposits with hyper-SW-AF. In this study, it was found that some of the deposits with hyper-IR-AF showed hypo-IR-AF after reattachment of the retina. This phenomenon occurred at the site of subretinal deposits showing hyper-SW-AF (Fig. 1). We hypothesize that lipofuscin-like materials may reduce IR-AF. A2E and its derivatives are known to elicit photooxidation in the RPE cells[37–40] and thereby reduce the amount of melanin in the RPE cells,[19,41–43] which, could cause a reduction in IR-AF. Furthermore, upregulation of oxidative stress in the RPE cells due to decreased melanin may facilitate apoptosis of the RPE. Of note, the final BCVA in the eyes observed for more than 6 months decreased in the eyes with granular hypo-IR-AF suggesting that the dysfunction of the RPE cells can affect the visual function.

The limitation of our study is that increasing IR-AF by melanogenesis and photo-oxidation have not been shown in a living human eye. Also, the magnitude of IR-AF induced by melanogenesis or photooxidation in vivo may not be enough to be detected by HRA2. Since the IR-AF contains AF generated from the choroidal tissue and is attenuated by the lesions of the retina, we may take the condition of the choroid and overlaying retina into consideration when we interpret IR-AF images. In conclusion, the IR-AF findings in CSC can be explained hypothetically by the modification of melanin in the RPE (Fig. 9). Regarding this hypothesis, we must be aware that the source of IR-AF remains unknown and future mechanistic studies are needed to validate this notion. Since IR-AF indicates the presence of the RPE, IR-AF can be used as a biomarker for the retinal pigment epithelial cells. IR-AF in combination with SW-AF may be useful to identify the cells participating in retinal lesions. In addition, as the intensity of IR-AF can be reduced by oxidative stress to the RPE, application of IR-AF for age-related macular degeneration may provide useful information. IR-AF can be an effective tool for investigating the RPE and the retina noninvasively.

References

1. Gass JD. Pathogenesis of disciform detachment of the neuroepithelium. *Am J Ophthalmol.* 1967;63:(suppl):1–139.
2. Jalkh AE, Jabbour N, Avila MP, Trempe CL, Schepens CL. Retinal pigment epithelium decompensation. I. Clinical features and natural course. *Ophthalmology.* 1984;91:1544–1548.
3. Yannuzzi LA, Shakin JL, Fisher YL, Altomonte MA. Peripheral retinal detachments and retinal pigment epithelial atrophic tracts secondary to central serous pigment epitheliopathy. *Ophthalmology.* 1984;91:1554–1572.
4. Levine R, Brucker AJ, Robinson F. Long-term follow-up of idiopathic central serous chorioretinopathy by fluorescein angiography. *Ophthalmology.* 1989;96:854–859.
5. Guyer DR, Yannuzzi LA, Slakter JS, Sorenson JA, Ho A, Orlock D. Digital indocyanine green videoangiography of central serous chorioretinopathy. *Arch Ophthalmol.* 1994;112:1057–1062.
6. Piccolino FC, Borgia L, Zinicola E, Zingirian M. Indocyanine green angiographic findings in central serous chorioretinopathy. *Eye.* 1995;9:324–332.
7. Iida T, Kishi S, Hagimura N, Shimizu K. Persistent and bilateral choroidal vascular abnormalities in central serous chorioretinopathy. *Retina.* 1999;19:508–512.
8. Iida T, Hagimura N, Sato T, Kishi S. Evaluation of central serous chorioretinopathy with optical coherence tomography. *Am J Ophthalmol.* 2000;129:16–20.
9. Maruko I, Iida T, Sekiryu T, Saito M. Morphologic changes in the outer layer of the detached retina in rhegmatogenous retinal detachment and central serous chorioretinopathy. *Am J Ophthalmol.* 2009;147:489–494.e481.
10. Ojima Y, Hangai M, Sasahara M, et al. Three-dimensional imaging of the foveal photoreceptor layer in central serous chorioretinopathy using high-speed optical coherence tomography. *Ophthalmology.* 2007;114:2197–2207.
11. Spaide RF, Klancnik JM Jr. Fundus autofluorescence and central serous chorioretinopathy. *Ophthalmology.* 2005;112:825–833.

12. Delori FC, Dorey CK, Staurenghi G, Arend O, Goger DG, Weiter JJ. In vivo fluorescence of the ocular fundus exhibits retinal pigment epithelium lipofuscin characteristics. *Invest Ophthalmol Vis Sci.* 1995;36:718-729.
13. Ben-Shabat S, Parish CA, Vollmer HR, et al. Biosynthetic studies of A2E, a major fluorophore of retinal pigment epithelial lipofuscin. *J Biol Chem.* 2002;277:7183-7190.
14. Krogmeier JR, Clancy CM, Pawlak A, et al. Mapping the distribution of emissive molecules in human ocular lipofuscin granules with near-field scanning optical microscopy. *J Microsc.* 2001;202:386-390.
15. Liu J, Itagaki Y, Ben-Shabat S, Nakanishi K, Sparrow JR. The biosynthesis of A2E, a fluorophore of aging retina, involves the formation of the precursor, A2-PE, in the photoreceptor outer segment membrane. *J Biol Chem.* 2000;275:29354-29360.
16. Kim SR, Nakanishi K, Itagaki Y, Sparrow JR. Photooxidation of A2-PE, a photoreceptor outer segment fluorophore, and protection by lutein and zeaxanthin. *Exp Eye Res.* 2006;82:828-839.
17. Framme C, Walter A, Gabler B, Roider J, Sachs HG, Gabel VP. Fundus autofluorescence in acute and chronic-recurrent central serous chorioretinopathy. *Acta Ophthalmol Scand.* 2005;83:161-167.
18. Kon Y, Iida T, Maruko I, Saito M. The optical coherence tomography-ophthalmoscope for examination of central serous chorioretinopathy with precipitates. *Retina.* 2008;28:864-869.
19. Sarna T, Burke JM, Korytowski W, et al. Loss of melanin from human RPE with aging: possible role of melanin photooxidation. *Exp Eye Res.* 2003;76:89-98.
20. Weinberger AW, Lappas A, Kirschkamp T, et al. Fundus near infrared fluorescence correlates with fundus near infrared reflectance. *Invest Ophthalmol Vis Sci.* 2006;47:3098-3108.
21. Keilhauer CN, Delori FC. Near-infrared autofluorescence imaging of the fundus: visualization of ocular melanin. *Invest Ophthalmol Vis Sci.* 2006;47:3556-3564.
22. Sekiryu T, Iida T, Maruko I, Horiguchi M. Clinical application of autofluorescence densitometry using a scanning laser ophthalmoscope. *Invest Ophthalmol Vis Sci.* 2009;50(6):2994-3002.
23. Feeney L. Lipofuscin and melanin of human retinal pigment epithelium. Fluorescence, enzyme cytochemical, and ultrastructural studies. *Invest Ophthalmol Vis Sci.* 1978;17:583-600.
24. Beatty S, Koh H, Phil M, Henson D, Boulton M. The role of oxidative stress in the pathogenesis of age-related macular degeneration. *Surv Ophthalmol.* 2000;45:115-134.
25. Hu DN, Simon JD, Sarna T. Role of ocular melanin in ophthalmic physiology and pathology. *Photochem Photobiol.* 2008;84:639-644.
26. Rozanowska M, Jarvis-Evans J, Korytowski W, Boulton ME, Burke JM, Sarna T. Blue light-induced reactivity of retinal age pigment: in vitro generation of oxygen-reactive species. *J Biol Chem.* 1995;270:18825-18830.
27. Ayata A, Tatlipinar S, Kar T, Unal M, Ersanli D, Bilge AH. Near-infrared and short-wavelength autofluorescence imaging in central serous chorioretinopathy. *Br J Ophthalmol.* 2009;93:79-82.
28. Dorey CK, Torres X, Swart T. Evidence of melanogenesis in porcine retinal pigment epithelial cells in vitro. *Exp Eye Res.* 1990;50:1-10.
29. Schraermeyer U. Does melanin turnover occur in the eyes of adult vertebrates? *Pigment Cell Res.* 1993;6:193-204.
30. Peters S, Kayatz P, Heimann K, Schraermeyer U. Subretinal injection of rod outer segments leads to an increase in the number of early-stage melanosomes in retinal pigment epithelial cells. *Ophthalmic Res.* 2000;32:52-56.
31. Julien S, Kociok N, Kreppel F, et al. Tyrosinase biosynthesis and trafficking in adult human retinal pigment epithelial cells. *Graefes Arch Clin Exp Ophthalmol.* 2007;245:1495-1505.
32. Matsumoto H, Kishi S, Otani T, Sato T. Elongation of photoreceptor outer segment in central serous chorioretinopathy. *Am J Ophthalmol.* 2008;145:162-168.
33. Miyamoto M, Fitzpatrick TB. On the nature of the pigment in retinal pigment epithelium. *Science.* 1957;126:449-450.
34. Sarna T. Properties and function of the ocular melanin: a photobiophysical view. *J Photochem Photobiol B.* 1992;12:215-258.
35. Smith-Thomas L, Richardson P, Thody AJ, et al. Human ocular melanocytes and retinal pigment epithelial cells differ in their melanogenic properties in vivo and in vitro. *Curr Eye Res.* 1996;15:1079-1091.
36. Kayatz P, Thumann G, Luther TT, et al. Oxidation causes melanin fluorescence. *Invest Ophthalmol Vis Sci.* 2001;42:241-246.
37. Zhang X, Zhou J, Fernandes AF, et al. The proteasome: a target of oxidative damage in cultured human retina pigment epithelial cells. *Invest Ophthalmol Vis Sci.* 2008;49:3622-3630.
38. Yakovleva MA, Sakina NL, Kononikhin AS, et al. Detection and study of the products of photooxidation of N-retinylidene-N-retinylethanolamine (A2E), the fluorophore of lipofuscin granules from retinal pigment epithelium of human donor eyes. *Dokl Biochem Biophys.* 2006;409:223-225.
39. Jang YP, Matsuda H, Itagaki Y, Nakanishi K, Sparrow JR. Characterization of peroxy-A2E and furan-A2E photooxidation products and detection in human and mouse retinal pigment epithelial cell lipofuscin. *J Biol Chem.* 2005;280:39732-39739.
40. Dontsov AE, Sakina NL, Golubkov AM, Ostrovsky MA. Light-induced release of A2E photooxidation toxic products from lipofuscin granules of human retinal pigment epithelium. *Dokl Biochem Biophys.* 2009;425:98-101.
41. Zareba M, Sarna T, Szewczyk G, Burke JM. Photobleaching of melanosomes from retinal pigment epithelium: II. Effects on the response of living cells to photic stress. *Photochem Photobiol.* 2007;83:925-930.
42. Zadlo A, Rozanowska MB, Burke JM, Sarna TJ. Photobleaching of retinal pigment epithelium melanosomes reduces their ability to inhibit iron-induced peroxidation of lipids. *Pigment Cell Res.* 2007;20:52-60.
43. Burke JM, Henry MM, Zareba M, Sarna T. Photobleaching of melanosomes from retinal pigment epithelium: I. Effects on protein oxidation. *Photochem Photobiol.* 2007;83:920-924.

Comparison of Intravitreal Triamcinolone Acetonide With Photodynamic Therapy and Intravitreal Bevacizumab with Photodynamic Therapy for Retinal Angiomatous Proliferation

MASAAKI SAITO, CHIEKO SHIRAGAMI, FUMIO SHIRAGA, MARIKO KANO, AND TOMOHIRO IIDA

• PURPOSE: To compare the efficacy of combined therapy with intravitreal triamcinolone (IVTA) and photodynamic therapy (PDT; IVTA plus PDT) with intravitreal bevacizumab (IVB) and PDT (IVB plus PDT) for patients with retinal angiomatous proliferation (RAP).

• DESIGN: Retrospective, observational case series.

• METHODS: We retrospectively reviewed 25 treatment-naïve eyes of 22 Japanese patients (11 men, 11 women) with retinal angiomatous proliferation. Twelve eyes of 11 patients were treated with combined therapy of IVTA plus PDT from September 1, 2004, through July 31, 2006. Thirteen eyes of 11 patients were treated with combined therapy of IVB plus PDT from February 1, 2007, through January 31, 2008.

• RESULTS: In 12 eyes treated with IVTA plus PDT, the mean best-corrected visual acuity (BCVA) levels at baseline and 12 months were 0.29 and 0.13, respectively. A significant ($P < .05$) decline in the mean BCVA from baseline was observed at 12 months. In 13 eyes treated with IVB plus PDT, the mean BCVA levels at baseline and 12 months were 0.25 and 0.37. A significant ($P < .05$) improvement in the mean BCVA from baseline was observed. At 12 months, the difference in BCVA between the 2 groups was significant ($P < .05$). The mean numbers of treatments at 12 months in the IVTA plus PDT group and the IVB plus PDT group were 2.7 and 1.6, respectively. The difference between the 2 treatments reached significance ($P < .05$). No complications developed.

• CONCLUSIONS: Compared with IVTA plus PDT, IVB plus PDT was significantly more effective in maintaining and improving visual acuity and in reducing the number of treatment for patients with retinal angiomatous proliferation. (Am J Ophthalmol 2010;149: 472–481. © 2010 by Elsevier Inc. All rights reserved.)

Accepted for publication Sep 21, 2009.

From the Department of Ophthalmology, Fukushima Medical University School of Medicine, Fukushima, Japan (M.S., M.K., T.I.); and the Department of Ophthalmology, Kagawa University, Kagawa, Japan (C.S., F.S.).

Inquiries to Masaaki Saito, Department of Ophthalmology, Fukushima Medical University School of Medicine, 1 Hikarigaoka, Fukushima 960-1295, Japan; e-mail: smasaaki@fmu.ac.jp

RETINAL ANGIOMATOUS PROLIFERATION (RAP) HAS been described as a variant of exudative age-related macular degeneration (AMD).[1] The term RAP was first coined by Yannuzzi and associates in 2001.[1] RAP is differentiated into 3 stages based on clinical and angiographic observations: stage 1, proliferation of intraretinal capillaries originating from the deep retinal complex (intraretinal neovascularization); stage 2, growth of the retinal vessels into the subretinal space (subretinal neovascularization); and stage 3, clinically or angiographically observed choroidal neovascularization (CNV).[1] RAP sometimes is referred to as type 3 neovascularization to distinguish it from the type 1 and 2 CNV anatomic classifications described by Freund and associates.[2]

RAP represents 15% of all neovascular AMD in white patients and 4.5% of all neovascular AMD in Japanese patients.[3,4] The natural course of RAP differs from typical exudative AMD and has poor visual outcomes.[5–7] Furthermore, various treatments for RAP such as conventional laser photocoagulation,[6,8] transpupillary thermotherapy,[6,9] surgical ablation,[10,11] and monotherapy of photodynamic therapy (PDT) with verteporfin (Visudyne; Novartis Pharma AG, Basel, Switzerland)[12,13] have not been efficacious.

CNV complexes are comprised of inflammatory cells and vascular endothelial growth factor (VEGF).[14–16] Corticosteroids such as triamcinolone acetonide (TA) have antiangiogenic, antiinflammatory, and anti-VEGF effects.[17,18] Recent studies have reported that combined therapy of intravitreal TA (IVTA) and PDT for RAP effectively resolves angiographic leakage and maintains or improves visual acuity (VA).[19,20]

Anti-VEGF therapy prevents formation of CNV and decreases leakage from existing CNV in animal models.[21] VEGF monoclonal antibodies and aptamers such as ranibizumab (Lucentis; Genentech, Inc, South San Francisco, California, USA), bevacizumab (Avastin; Genentech), and pegaptanib (Macugen; EyeTech Pharmaceuticals, Lexington, Massachusetts, USA) reduce vascular leakage and improve visual outcomes in patients with CNV secondary to AMD.[22–25] Moreover, combined therapy of intravitreal bevacizumab (IVB) injections and PDT administered to treat CNV reduced the retreatment rates in patients with AMD.[26–28] We reported recently that combined therapy of IVB and PDT was effective for treating RAP after 6

0002-9394/10/$36.00
doi:10.1016/j.ajo.2009.09.016

TABLE 1. Intravitreal Triamcinolone Acetonide and Photodynamic Therapy for Retinal Angiomatous Proliferation

						Baseline					12 Months after Treatment				
Case No.	Age (yrs)	Gender	Eye	RAP Stage	Lens Status	VA	Central Retinal Thickness (μm)	RRA	GLD (μm)	IOP (mmHg)	VA	Central Retinal Thickness (μm)	RRA	GLD (μm)	IOP (mmHg)	No. Treatments
1	74	F	Right	2+PED	Phakic eye	0.8	279	Yes	1590	13	0.8	34	No	0	12	1
2	85	F	Right	2	Pseudophakia	0.2	385	Yes	1100	13	0.1	115	Yes	0	11	2
3	86	M	Right	2	Phakic eye	0.4	293	Yes	2570	10	0.1	550	Yes	2197	10	4
4	86	M	Left	2+PED	Phakic eye	0.3	350	Yes	1080	11	0.2	289	Yes	957	11	4
5	74	F	Left	2	Pseudophakia	0.8	542	Yes	3600	13	0.5	232	No	0	12	3
6	63	M	Right	2+PED	Phakic eye	0.8	267	Yes	5610	17	0.06	481	Yes	4784	18	3
7	84	F	Right	2+PED	Phakic eye	0.6	355	Yes	2690	10	0.08	407	Yes	3296	9	5
8	90	F	Right	2	Pseudophakia	0.3	314	No	4516	13	0.03	83	—	0	16	1
9	70	F	Left	2	Pseudophakia	0.09	367	Yes	2450	16	0.2	324	Yes	0	19	2
10	69	F	Right	2	Phakic eye	0.15	625	Yes	3334	14	0.1	135	Yes	0	10	3
11	68	M	Right	2	Pseudophakia	0.1	521	Yes	3430	20	0.3	237	Yes	0	16	2
12	90	F	Right	2+PED	Pseudophakia	0.1	575	Yes	2648	14	0.05	423	Yes	0	15	2
Mean	78	—	—	—	—	0.29	406	—	2885	13.7	0.13	276	—	936	13.3	2.7
SD	9.5	—	—	—	—	—	125	—	1335	2.9	—	166	—	1623	3.4	1.2

F = female; GLD = greatest linear dimension; IOP = intraocular pressure; M = male; PED = pigment epithelial detachment; RAP = retinal angiomatous proliferation; RRA = retinal–retinal anastomosis; SD = standard deviation; VA = decimal visual acuity; yrs = years.

TABLE 2. Intravitreal Bevacizumab and Photodynamic Therapy for Retinal Angiomatous Proliferation

						Baseline					12 Months after Treatment				
Case No.	Age (yrs)	Gender	Eye	RAP Stage	Lens Status	VA	Central Retinal Thickness (μm)	RRA	GLD (μm)	IOP (mmHg)	VA	Central Retinal Thickness (μm)	RRA	GLD (μm)	IOP (mmHg)	No. Treatments
13	64	F	Right	2	Phakic eye	1.0	234	No	602	16	1.0	117	—	0	12	2
14	63	M	Right	2+PED	Phakic eye	0.07	601	Yes	4331	12	0.2	126	No	0	10	2
15	81	M	Right	2	Phakic eye	0.4	393	No	1900	15	1.0	124	—	0	13	1
16	78	M	Left	2	Phakic eye	0.6	406	No	1998	11	1.2	125	—	0	11	1
17	89	M	Left	2+PED	Pseudophakia	0.3	379	Yes	3531	16	0.6	182	No	0	13	1
18	87	F	Right	3	Pseudophakia	0.06	394	Yes	2368	10	0.07	140	Yes	0	10	1
19	87	F	Left	2+PED	Pseudophakia	0.7	396	Yes	5532	10	0.7	112	Yes	0	10	2
20	78	M	Left	2	Phakic eye	0.9	430	Yes	975	15	0.8	127	No	0	14	2
21	83	F	Right	2	Phakic eye	0.05	514	Yes	3489	19	0.05	88	No	0	14	2
22	83	F	Left	2+PED	Pseudophakia	0.3	479	Yes	4568	17	0.6	44	No	0	16	3
23	72	M	Right	2+PED	Phakic eye	0.3	360	Yes	3300	16	0.2	74	No	0	13	2
24	74	M	Right	3	Phakic eye	0.06	950	Yes	4494	15	0.09	426	No	0	11	1
25	79	M	Left	2+PED	Pseudophakia	0.3	389	Yes	3321	11	0.9	66	No	0	10	1
Mean	78	—	—	—	—	0.25	456	—	3108	14.1	0.37	135	—	0	12.1	1.6
SD	8.2	—	—	—	—	—	171	—	1469	2.9	—	94	—	—	1.9	0.7

F = female; GLD = greatest linear dimension; M = male; PED = pigment epithelial detachment; RAP = retinal angiomatous proliferation; RRA = retinal–retinal anastomosis; SD = standard deviation; VA = decimal visual acuity; yrs = years.

months of follow-up.[29] The purpose of the current study was to clarify the efficiency of combined therapy of IVB plus PDT compared with combined therapy of IVTA plus PDT for treating patients with RAP over 12 months.

METHODS

WE RETROSPECTIVELY REVIEWED 25 EYES OF 22 JAPANESE patients (11 men, 11 women; age range, 63 to 90 years; mean ± standard deviation, 78.3 ± 8.8 years) with RAP. Twelve eyes of 11 patients (3 men, 8 women; age range, 63 to 90 years; mean age, 78.3 years) were treated with combined therapy of IVTA plus PDT from September 1, 2004, through July 31, 2006. Thirteen eyes of 11 patients (8 men, 3 women; age range, 63 to 89 years; mean age, 78.3 years) were treated with combined therapy of IVB and PDT from February 1, 2007, through January 31, 2008. The 6-month results for 8 of the 13 eyes treated with IVB plus PDT were reported previously.[29] The patients were followed up for at least 12

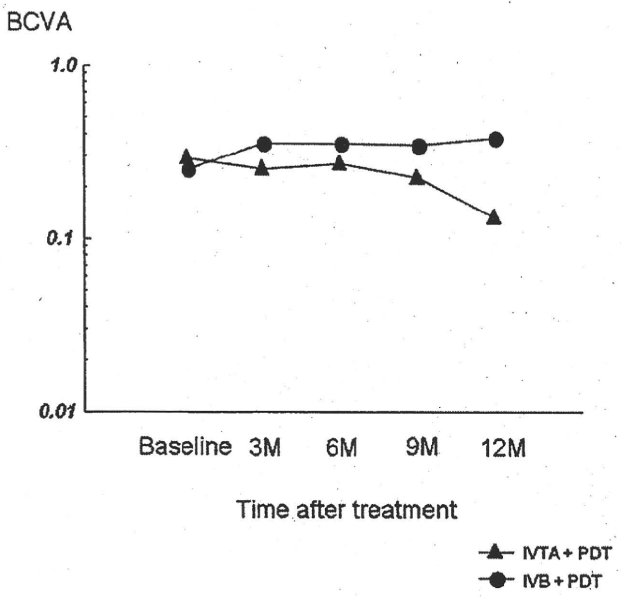

FIGURE 1. Graph showing results of intravitreal triamcinolone acetonide with photodynamic therapy (IVTA plus PDT) and intravitreal bevacizumab with photodynamic therapy (IVB plus PDT) for retinal angiomatous proliferation (RAP). In eyes treated with IVTA plus PDT, there is a significant ($P < .05$, paired t test) decline in the mean best-corrected visual acuity (BCVA) between baseline and 12 months. In eyes treated with IVB plus PDT, there is a significant improvement in the mean BCVA between baseline and 3, 6, and 12 months ($P < .01$, $P < .05$, $P < .05$, respectively, paired t test). There is no significant ($P = .74$) difference in the mean BCVA between groups at baseline; nevertheless, there is a significant difference in the mean BCVA at 12 months ($P < .05$, nonpaired t test) between the IVB plus PDT group and the IVTA plus PDT group. M = month(s).

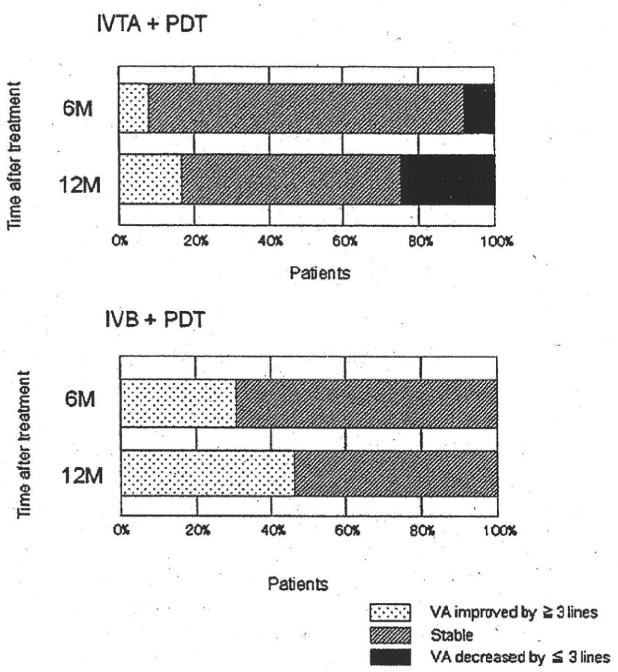

FIGURE 2. The distribution of the mean best-corrected visual acuity (BCVA) changes from baseline after treatment with combined intravitreal triamcinolone acetonide with photodynamic therapy (IVTA plus PDT) and intravitreal bevacizumab with photodynamic therapy (IVB plus PDT). (Top) One and 3 eyes treated with IVTA plus PDT had decreased BCVA at 6 and 12 months, respectively. (Bottom) No eyes treated with IVB plus PDT had decreased BCVA of 3 lines or more after treatment over 12 months. M = month(s).

months at Fukushima Medical University Hospital or Kagawa University Hospital. No patient had undergone a previous treatment. The treatment was approved by the Institutional Review Boards/Ethics Committees at Fukushima Medical University and Kagawa University. After the potential risks and benefits were explained in detail, all patients provided written informed consent. The exclusion criteria were previous treatment for RAP such as laser photocoagulation, submacular surgery, transpupillary thermotherapy, and PDT; glaucoma; tears in the retinal pigment epithelium; and maculopathies such as diabetic maculopathy, retinal vascular occlusion, or idiopathic juxtafoveal retinal telangiectasis.

We recorded the best-corrected visual acuity (BCVA) measured with a Japanese standard decimal VA chart and calculated the mean BCVA using the logarithm of the minimal angle of resolution (logMAR) scale. All patients underwent a standardized examination including slit-lamp biomicroscopy with a contact lens, fundus color photography, fluorescein angiography (FA), and indocyanine green angiography (ICGA) with a fundus camera (TRC-50 FA/IA/IMAGEnet H1024 system; Topcon, Tokyo, Japan), with a confocal scanning laser ophthalmoscope (Heidelberg Retina Angiograph 2; Heidelberg Engineering, Heidelberg, Germany), or both. All examinations were performed using time-domain optical coherence tomography (OCT; OCT 3000; Carl Zeiss, Meditec, Dublin, California, USA; or OCT-Ophthalmoscope; Nidek-OTI, Gamagori, Japan) in eyes treated with IVTA plus PDT and spectral-domain OCT (3D-OCT; Topcon; or Cirrus OCT, Carl Zeiss) in eyes treated with IVB plus PDT. All patients were examined using the same OCT machine during the follow-up. FA was performed to determine the lesion type, the location, and the activity of the RAP lesions. ICGA was performed to diagnose RAP and to identify retinal–retinal anastomosis. The central retinal thickness, defined as the distance from the retinal pigment epithelium to the inner limiting membrane, was measured at baseline and at 3, 6, 9, and 12 months after treatment using internal caliper software.

All patients had documented visual loss before treatment. IVTA (4 mg/0.1 mL) or IVB (1.25 mg/0.05 mL) was injected 3.5 to 4.0 mm posterior to the corneal limbus into the vitreous cavity using a 27-gauge needle after topical anesthesia was applied. In the patients treated with IVTA plus PDT, PDT was performed 7 days after IVTA was injected. In the patients treated with IVB plus PDT, PDT was administered 1

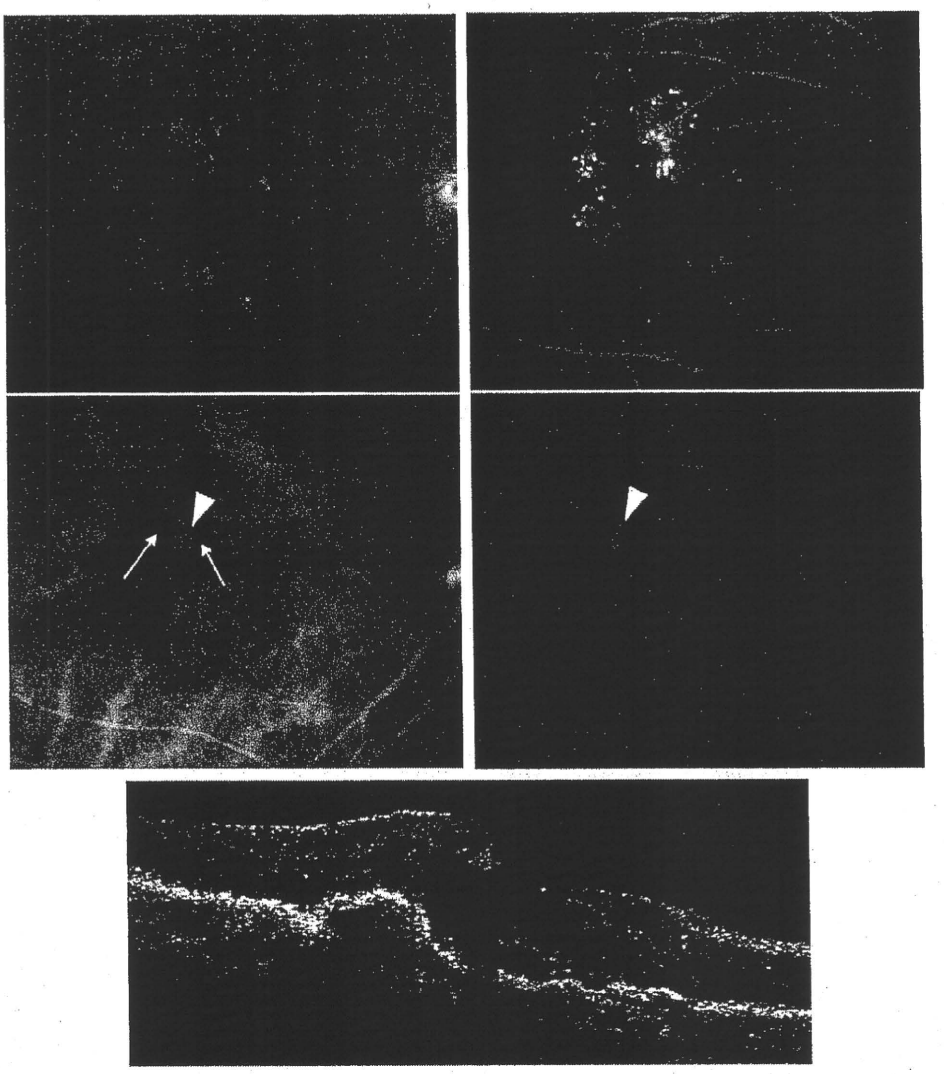

FIGURE 3. Case 7: an 84-year-old woman was treated with combined intravitreal triamcinolone acetonide with photodynamic therapy (IVTA plus PDT) for stage 2 retinal angiomatous proliferation (RAP) with a pigment epithelial detachment (PED). At baseline, the best-corrected visual acuity (BCVA) was 0.6 decimal VA in the right eye with stage 2 RAP. (Top left) Red-free photograph showing small intraretinal and preretinal hemorrhages, a PED, and drusen. (Top right) Fluorescein angiogram showing leakage and intraretinal edema. (Middle left) Early-phase indocyanine green angiogram (ICGA) showing retinal-retinal anastomosis (arrows) and a RAP lesion (arrowhead). (Middle right) Late-phase ICGA showing a focal area of intense hyperfluorescence (hot spot; arrowhead). (Bottom) Baseline horizontal optical coherence tomography image showing cystoid macular edema and a PED. Photodynamic therapy was applied (laser spot size, 3700 μm) 1 week after IVTA.

or 2 days after IVB was injected. PDT with verteporfin was administered according to the protocol of the Treatment of Age-Related Macular Degeneration with Photodynamic Therapy study.[30] A 689-nm laser system (Carl Zeiss Meditec) was used and 50 J/cm^2 energy was delivered with an 83-second exposure time. The greatest linear dimension (GLD) was measured based on FA findings. The laser spot size was determined by FA (FA-guided PDT) in 20 eyes and by ICGA (ICGA-guided PDT) in 5 eyes. FA-guided PDT was performed for the entire lesion seen on FA. ICGA-guided PDT was chosen if the lesion comprised a larger subretinal hemorrhage at least 1 disc diameter in size.

All patients were examined 3, 6, 9, and 12 months after the initial PDT was administered. Statistical analysis was performed using the Student *t* test to compare the VA and the central retinal thickness 3, 6, 9, and 12 months from baseline.

RESULTS

TABLES 1 AND 2 SHOW THE CHARACTERISTICS AND CLINICAL data of the 22 patients (25 eyes) at baseline and after treatment. All patients were Japanese and were observed

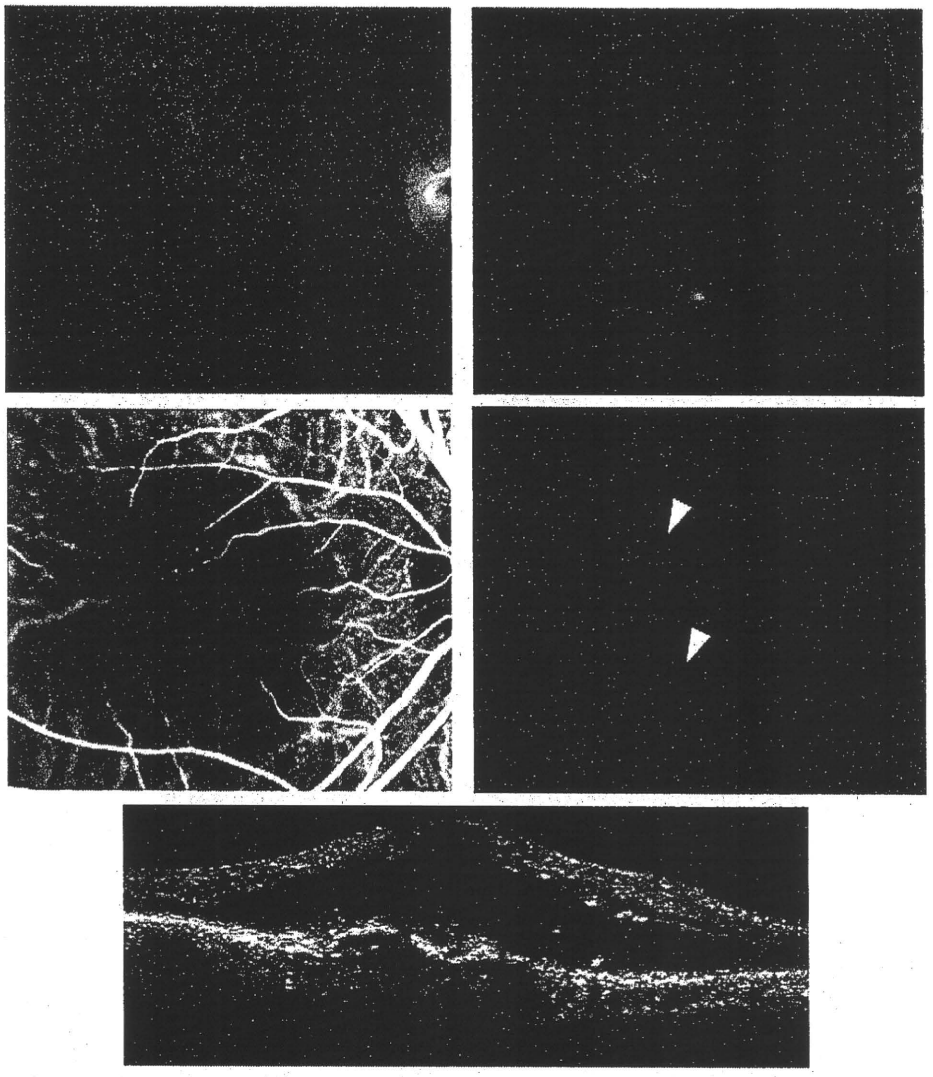

FIGURE 4. Case 7: 12 months after combined intravitreal triamcinolone acetonide with photodynamic therapy (IVTA plus PDT). Four treatments with combined therapy of IVTA plus PDT were administered over 12 months. The best-corrected visual acuity (VA) declined from 0.6 to 0.08 decimal VA. (Top left and right) Fluorescein angiograms showing that a hemorrhage, a shallow pigment epithelial detachment (PED), and leakage remain. (Middle left and right) Indocyanine green angiogram showing persistent and new retinal-retinal anastomosis and hot spots (arrowheads). (Bottom) Horizontal optical coherence tomography image showing persistent cystoid macular edema and a PED. A fifth treatment was administered.

for 12 months. There was no difference in the mean age between the 2 groups. In the 12 eyes treated with IVTA plus PDT, 7 eyes had stage 2 RAP without a retinal pigment epithelial detachment (PED) and 5 eyes had stage 2 RAP with a PED. In the 13 eyes treated with IVB plus PDT, 5 eyes had stage 2 RAP without a PED, 6 eyes had stage 2 RAP with a PED, and 2 eyes had stage 3 RAP. The mean GLD of the entire lesion was 2670 μm. There was no significant difference in the baseline patient characteristics between the 2 treatment groups.

In the 12 eyes treated with IVTA plus PDT, the mean BCVA levels at baseline and 3, 6, 9, and 12 months after treatment were 0.29, 0.25, 0.27, 0.22, and 0.13, respectively (Figure 1), indicating a significant ($P < .05$, paired t test) decline in the mean BCVA from baseline at 12 months. The mean changes in the BCVA at 6 and 12 months from baseline were a decline of 0.19 and 3.28 lines, respectively. One of the 12 eyes (8.3%) had an increase in the BCVA of 3 lines or more, 10 eyes (83.4%) had stable VA, and 1 eye (8.3%) had a decrease in the BCVA of 3 lines or more 6 months from baseline. At 12 months, 2 (16.7%) of 12 eyes had an increase in the BCVA of 3 lines or more, 7 eyes (58.3%) had stable VA, and 3 eyes (25%) had a decrease in the BCVA of 3 lines or more from baseline (Figure 2). The central retinal thickness significantly ($P < .05$, paired t test) decreased from baseline from 406 ± 125 μm (mean ± standard deviation) to 287 ± 124 μm at 3 months, 274 ± 174 μm at 6 months, 261 ± 208

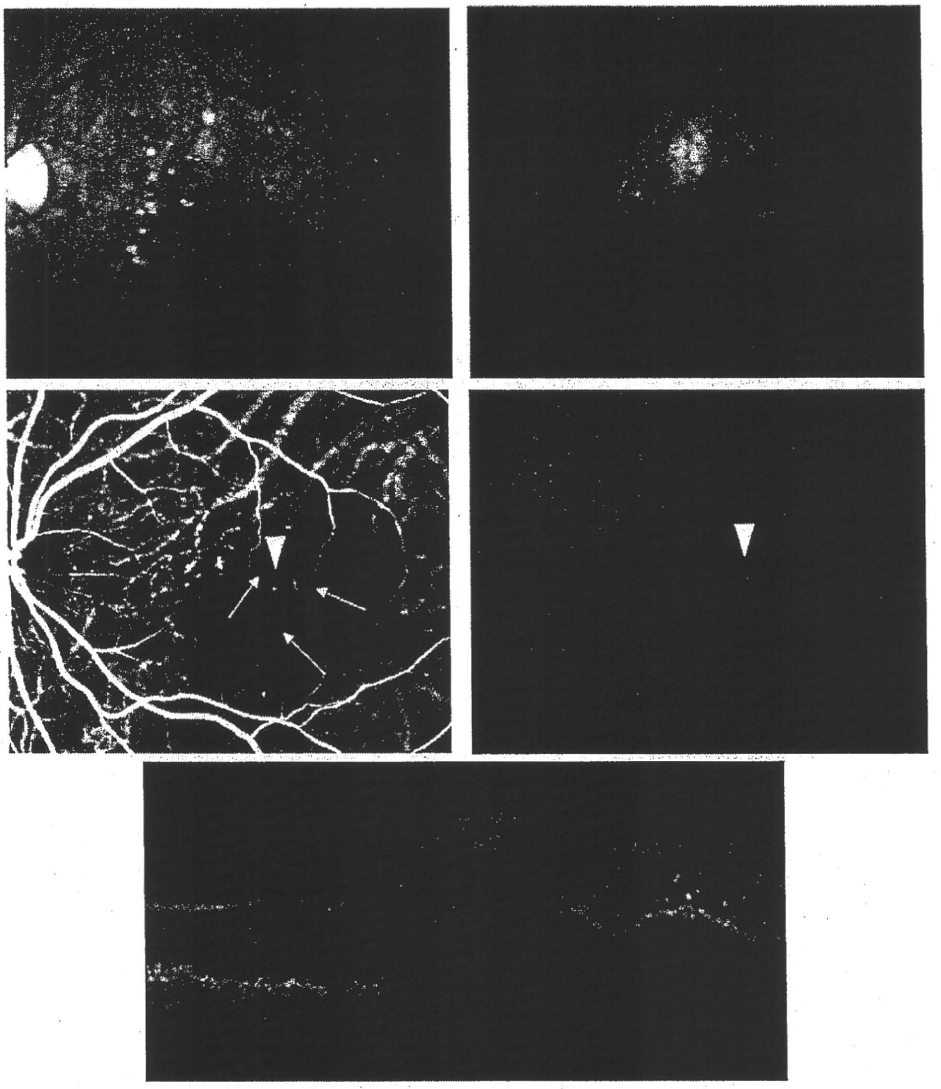

FIGURE 5. Case 22: an 83-year-old woman was treated with combined therapy of intravitreal bevacizumab and photodynamic therapy (IVB plus PDT) for stage 2 retinal angiomatous proliferation (RAP) with a pigment epithelial detachment (PED). At baseline, the best-corrected visual acuity (VA) was 0.3 decimal VA in the left eye with stage 2 RAP with a PED. (Top left) Red-free photograph showing small intraretinal and preretinal hemorrhages, a PED, and drusen. (Top right) Fluorescein angiogram showing leakage and intraretinal edema. (Middle left) Early-phase indocyanine green angiogram (ICGA) showing retinal-retinal anastomosis (arrows) and a RAP lesion (arrowhead). (Middle right) Late-phase ICGA showing a focal area of intense hyperfluorescence (hot spot; arrowhead). (Bottom) Baseline vertical optical coherence tomography image showing cystoid macular edema and a PED. Photodynamic therapy was applied (laser spot size, 5600 μm) 2 days after IVB.

μm at 9 months, and 276 ± 166 μm at 12 months. At baseline, cystoid macular edema (CME) was observed in 11 of the 12 eyes; there was a serous retinal detachment (SRD) in 7 of the 12 eyes, and a PED in 5 of the 12 eyes. The CME resolved in 5 (45.5%) eyes a mean of 5.4 weeks after baseline and decreased in 6 eyes. The SRD resolved completely in 5 (71.4%) eyes a mean of 3.1 weeks after baseline and decreased in 2 eyes. The PED resolved completely in 2 (40%) eyes a mean of 6.5 weeks after baseline and remained in 3 eyes. The mean GLD of the entire lesion was 2885 μm at baseline and 936 μm at 12 months ($P = .06$ compared with baseline). Six eyes were phakic and 6 eyes were pseudophakia. The mean intraocular pressure (IOP) was 13.7 mm Hg at baseline and 13.3 mm Hg at 12 months. Figures 3 and 4 show ocular images obtained from a patient treated with IVTA plus PDT.

In the 13 eyes treated with IVB plus PDT, the mean BCVA levels at baseline and 3, 6, 9, and 12 months after treatment were 0.25, 0.35, 0.35, 0.34, and 0.37, respectively (Figure 1). A significant improvement in the mean BCVA from baseline was seen at 3, 6, and 12 months ($P < .01$, $P < .05$, $P < .05$, respectively, paired t test; Figure 1).

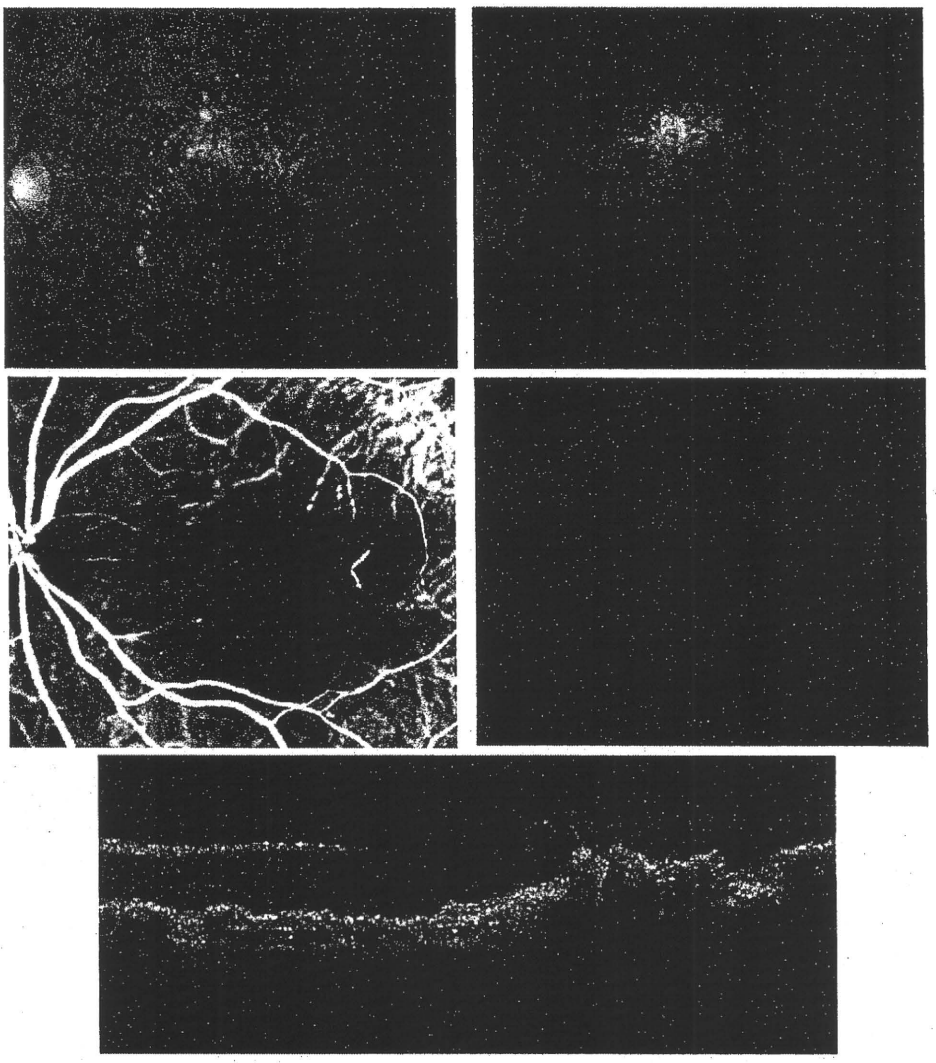

FIGURE 6. Case 22: 12 months after combined therapy of intravitreal bevacizumab and photodynamic therapy (IVB plus PDT). Three treatments were administered over 12 months. The best-corrected visual acuity (VA) improved from 0.3 to 0.6 decimal VA. (Top left and right) Fluorescein angiogram showing no hemorrhages, pigment epithelial detachment (PED), or leakage. (Middle left and right) Indocyanine green angiogram showing clear resolution of the retinal-retinal anastomosis and a hot spot. (Bottom) Vertical optical coherence tomography image showing absorption of the cystoid macular edema and a PED.

Although there was no significant difference in the mean BCVA at baseline between the 2 treatment groups ($P = .74$), there was a significant difference in the mean BCVA at 12 months ($P < .05$, nonpaired t test; Figure 1). The mean changes in BCVA at 6 and 12 months from baseline were improvements of 1.46 and 1.73 lines, respectively. The mean changes in BCVA at 3, 6, and 12 months were significantly better in the IVB plus PDT group than in the IVTA plus PDT group ($P < .05$, $P < .05$, $P < .01$, respectively, using the nonpaired t test). Four (30.8%) of the 13 eyes had an increase in the BCVA of 3 lines or more, and 9 eyes (69.2%) had stable VA at 6 months. At 12 months, 6 (46%) of 13 eyes had an increase in the BCVA of 3 lines or more, and 7 eyes (54%) had stable VA from baseline (Figure 2). No patient had decreased BCVA of 3 lines or more after treatment during any 12 months. The central retinal thickness decreased significantly from 456 ± 171 μm at baseline to 229 ± 213 μm at 3 months ($P < .01 \times 10^{-3}$), 233 ± 162 μm at 6 months ($P < .01 \times 10^{-5}$), 164 ± 120 μm at 9 months ($P < .01 \times 10^{-3}$), and 135 ± 94 μm at 12 months ($P < .01 \times 10^{-4}$). At baseline, all 13 eyes had CME, 8 of the 13 eyes had an SRD, and 8 of the 13 eyes had a PED. The CME resolved in 11 (84.6%) eyes a mean of 2.4 weeks after baseline and decreased in 2 eyes. The SRD resolved in 7 (87.5%) eyes 3.9 weeks after baseline and decreased in 1 eye. The PED resolved in 4 (50%) eyes a mean of 4.4 weeks after baseline and decreased in 3 eyes. The mean GLD of the entire lesion was 3108 μm at baseline and 0 μm at 12 months ($P < .01 \times 10^{-3}$, compared with baseline). Eight eyes

were phakic and 5 eyes were pseudophakia. The mean IOP was 14.1 mm Hg at baseline and 12.1 mm Hg at 12 months. Figures 5 and 6 show ocular images obtained from a patient treated with IVB plus PDT. The mean numbers of treatments at 12 months in the IVTA plus PDT and IVB plus PDT groups were 2.7 and 1.6, respectively, a difference that reached significance ($P < .05$, nonpaired t test). At the 12-month follow-up, FA showed resolution of leakage in all eyes treated with IVB plus PDT and resolution of leakage in 8 of the 12 eyes treated with IVTA plus PDT; the remaining 4 eyes underwent retreatments for persistent leakage.

At baseline, early-phase ICGA identified retinal–retinal anastomosis in 11 of 12 eyes treated with IVTA plus PDT and in 10 of 13 eyes treated with IVB plus PDT. Three months after treatment, complete occlusion of the retinal–retinal anastomosis was achieved in 1 (9.1%) of the 11 eyes treated with IVTA plus PDT and in 6 (60%) of the 10 eyes treated with IVB plus PDT. Among the remaining eyes (10 eyes treated with IVTA plus PDT and 4 eyes treated with IVB plus PDT) without occlusion of the retinal–retinal anastomosis, early-phase ICGA showed that the retinal–retinal anastomosis had narrowed in 1 of the 10 eyes treated with IVTA plus PDT and in all 4 eyes treated with IVB plus PDT. Moreover, 12 months after the initial treatment, complete occlusion of the retinal–retinal anastomosis was achieved in 2 (18.2%) of the 11 eyes treated with IVTA plus PDT and in 8 (80%) of the 10 eyes treated with IVB plus PDT.

Late-phase ICGA at baseline showed a hot spot in 11 of 12 eyes treated with IVTA plus PDT and in 12 of 13 eyes treated with IVB plus PDT. In 3 (27.2%) of the 11 eyes treated with IVTA plus PDT and in 100% of the 13 eyes treated with IVB plus PDT, the hot spot resolved 3 months after treatment. Moreover, 12 months after the initial treatment, the hot spot resolved in 2 (18.2%) of the 11 eyes treated with IVTA plus PDT and in 100% of the 13 eyes treated with IVB plus PDT. No complications, such as inflammation, increases in IOP to more than 21 mm Hg, severe vision loss, endophthalmitis, progression of cataract, or systemic events, developed.

DISCUSSION

THE CURRENT STUDY SHOWED THAT COMBINED TREATMENT of IVB plus PDT significantly improved the VA and reduced the number of treatments in patients with RAP compared with combined treatment of IVTA plus PDT during a 12-month follow-up.

The natural course of RAP has been reported to have poor visual outcomes compared with that of typical AMD.[5–7] The general consensus is that the disease is associated with a poor functional prognosis and resultant disciform scarring.[1,6,7] Conventional laser photocoagulation,[6,8] transpupillary thermotherapy,[6,9] surgical ablation,[10,11,30] and PDT alone[12,13] have been used to treat patients with RAP. However, poor visual outcomes usually result from these monotherapies.[6,8–13]

We reported the efficacy of IVB plus PDT for treating RAP with 6 months of follow-up.[29] In the current study, we found a significant ($P < .05$, paired t test) improvement in the mean BCVA from baseline at 12 months. The BCVA in 6 (46%) of 13 eyes increased by 3 lines or more, and 7 eyes (54%) had stable VA.

An inflammatory response and upregulation of VEGF have been reported after application of PDT.[31,32] TA has antiangiogenic, antiinflammatory, and anti-VEGF effects.[17,18] Combination therapy of PDT and TA reduced the inflammatory response and upregulation of VEGF associated with CNV and PDT. Freund and associates reported that combination therapy of IVTA plus PDT reduced or eliminated edema, achieved rapid regression of neovascularization, and stabilized or improved VA in white patients with RAP.[19] Those authors speculated that verteporfin may leak into the retinal cystic spaces, and to avoid predisposing the retinal layers to photochemical damage, they applied PDT 1 week after IVTA (referred to as pharmacology-pause-PDT). Because this method was well conceived, we administered IVTA plus PDT accordingly. Nevertheless, a significant ($P < .05$, paired t test) decline in the mean BCVA from baseline was observed at 12 months. The reason why pharmacology-pause-PDT was ineffective for treating Japanese patients in the current study is unknown.

Intraretinal neovascularization, subretinal neovascularization, and retinal–retinal anastomosis are evidence of RAP lesions.[1] Surgical lysis of the feeding arterioles and draining venules was effective because it eliminated high-flow blood supply to the RAP lesions.[33] Achieving complete occlusion of the retinal–retinal anastomosis is important for reducing RAP lesions. In patients with RAP, several injections of IVB monotherapy were needed but did not achieve complete occlusion of the feeder vessels.[34,35] We reported the efficacy of IVB plus PDT for RAP for achieving complete occlusion of retinal–retinal anastomosis during a 6-month follow-up.[29] In the current study, complete occlusion of the retinal–retinal anastomosis was achieved in 2 (18.2%) of the 11 eyes treated with IVTA plus PDT and in 8 (80%) of the 10 eyes treated with IVB plus PDT 12 months after treatment. IVB plus PDT can reduce the high-flow blood supply to RAP lesions over a long period.

Rouvas and associates compared ranibizumab, ranibizumab combined with PDT, and IVTA plus PDT with a minimum 6-month follow-up.[20] In that report, the mean VA at baseline to the end of the follow-up decreased from 0.83 to 0.85 logMAR in eyes treated with ranibizumab, decreased from 0.61 to 0.63 logMAR in eyes treated with ranibizumab plus PDT, and improved from 0.92 to 0.61 logMAR ($P = .183$) in eyes treated with IVTA plus PDT. The authors concluded that all therapies resulted in

stabilized disease, whereas IVTA plus PDT achieved better functional and anatomic results compared with the other treatments. In the current study, the mean BCVA improved significantly from 0.25 at baseline to 0.37 at 12 months in eyes treated with IVB plus PDT ($P < .05$). The investigators suggested that bevacizumab has a longer half-life than ranibizumab, so they did not observe any differences in ranibizumab and ranibizumab in combination with PDT as when using bevacizumab.

We performed PDT 1 or 2 days after administering IVB. Overexpression of VEGF in the retina (photoreceptors) is sufficient to cause intraretinal and subretinal neovascularization in animal models,[36] which is similar to the neovascular process of RAP. Using injections of intravitreal anti-VEGF agents combined with PDT is reasonable for inhibiting VEGF-induced PDT and the neovascularization of RAP. Rouvas and associates administered PDT 7 ± 2 days after ranibizumab was injected intravitreously.[20] The ideal interval between intravitreal injection of anti-VEGF agents and PDT is unknown and remains controversial. Freund and associates reported that 1 intravitreal ranibizumab injection to treat RAP resulted in rapid resolution of the intraretinal edema, hemorrhage, and neovascular lesions.[2] In typical AMD eyes, the central retinal thickness measurements decreased immediately after injection of ranibizumab.[37,38] The clinical efficacy may depend on the suppression of CNV using anti-VEGF agents. Verteporfin may accumulate minimally in the suppressed neovascular complex after injection of intravitreal anti-VEGF agents. For this reason, we applied PDT as soon as possible after IVB. Applying PDT simultaneously with intravitreal anti-VEGF agents also may be effective.

Development of complications after PDT, such as severe vision loss of approximately 4.5% in the first year[30] or the enlargement of the hypofluorescence on ICGA, has been reported.[39] The complications after IVTA include elevated IOP, progression of cataracts in phakic patients, and development of endophthalmitis.[40,41] In the current study, no patients had severe vision loss, IOP of more than 21 mm Hg, or cataract progression during the 12 months of follow-up.

In conclusion, the results of the current study indicate that combined therapy of IVB plus PDT was significantly more effective for maintaining or improving VA and reducing the number of treatments in patients with RAP compared with combined therapy of IVTA and PDT. Because this was a pilot study, larger and long-term prospective randomized studies are needed to determine the efficacy and safety profiles of combined bevacizumab or of an anti-VEGF agent and PDT.

THE AUTHORS INDICATE NO FINANCIAL SUPPORT OR FINANCIAL CONFLICT OF INTEREST. INVOLVED IN DESIGN AND conduct of study (M.S., T.I., F.S.); Collection, management, analysis, and interpretation of the data (M.S., C.S., M.K.); preparation, review, and revision of the manuscript (M.S., T.I.); and Approval of the manuscript (M.S., C.S., F.S., M.K., T.I.). The treatments in this study were approved by the Institutional Review Board/Ethics Committee of Fukushima Medical University and Kagawa University in Japan. After the potential risks and benefits were explained in detail, all patients provided written informed consent.

REFERENCES

1. Yannuzzi LA, Negrão S, Iida T, et al. Retinal angiomatous proliferation in age-related macular degeneration. Retina 2001;21:416–434.
2. Freund KB, Ho IV, Barbazetto IA, et al. Type 3 neovascularization: the expanded spectrum of retinal angiomatous proliferation. Retina 2008;28:201–211.
3. Cohen SY, Creuzot-Garcher C, Darmon J, et al. Types of choroidal neovascularisation in newly diagnosed exudative age-related macular degeneration. Br J Ophthalmol 2007;91:1173–1176.
4. Maruko I, Iida T, Saito M, Nagayama D, Saito K. Clinical characteristics of exudative age-related macular degeneration in Japanese patients. Am J Ophthalmol 2007;144:15–22.
5. Hartnett ME, Weiter JJ, Staurenghi G, Elsner AE. Deep retinal vascular anomalous complexes in advanced age-related macular degeneration. Ophthalmology 1996;103:2042–2053.
6. Bottoni F, Massacesi A, Cigada M, Viola F, Masicco I, Staurenghi G. Treatment of retinal angiomatous proliferation in age-related macular degeneration: a series of 104 cases of retinal angiomatous proliferation. Arch Ophthalmol 2005;123:1644–1650.
7. Bressler NM. Retinal anastomosis to choroidal neovascularization: a bum rap for a difficult disease. Arch Ophthalmol 2005;123:1741–1743.
8. Slakter JS, Yannuzzi LA, Schneider U, et al. Retinal choroidal anastomoses and occult choroidal neovascularization in age-related macular degeneration. Ophthalmology 2000;107:742–753.
9. Kuroiwa S, Arai J, Gaun S, Iida T, Yoshimura N. Rapidly progressive scar formation after transpupillary thermotherapy in retinal angiomatous proliferation. Retina 2003;23:417–420.
10. Sakimoto S, Gomi F, Sakaguchi H, Tano Y. Recurrent retinal angiomatous proliferation after surgical ablation. Am J Ophthalmol 2005;139:917–918.
11. Shiragami C, Iida T, Nagayama D, Baba T, Shiraga F. Recurrence after surgical ablation for retinal angiomatous proliferation. Retina 2007;27:198–203.
12. Boscia F, Furino C, Sborgia L, Reibaldi M, Sborgia C. Photodynamic therapy for retinal angiomatous proliferations and pigment epithelium detachment. Am J Ophthalmol 2004;138:1077–1079.
13. Silva RM, Cachulo ML, Figueira J, de Abreu JR, Cunha-Vaz JG. Chorioretinal anastomosis and photodynamic therapy: a two-year follow-up study. Graefes Arch Clin Exp Ophthalmol 2007;245:1131–1139.
14. Kvanta A, Algvere PV, Berglin L, Seregard S. Subfoveal fibrovascular membranes in age-related macular degeneration express vascular endothelial growth factor. Invest Ophthalmol Vis Sci 1996;37:1929–1934.

15. Kliffen M, Sharma HS, Mooy CM, Kerkvliet S, de Jong PT. Increased expression of angiogenic growth factors in age-related maculopathy. Br J Ophthalmol 1997;81:154–162.
16. Oh H, Takagi H, Takagi C. The potential angiogenic role of macrophages in the formation of choroidal neovascular membranes. Invest Ophthalmol Vis Sci 1999;40:1891–1898.
17. Penfold PL, Wen L, Madigan MC, King NJ, Provis JM. Modulation of permeability and adhesion molecule expression by human choroidal endothelial cells. Invest Ophthalmol Vis Sci 2002;43:3125–3130.
18. Hori Y, Hu DE, Yasui K, Smither RL, Gresham GA, Fan TP. Differential effects of angiostatic steroids and dexamethasone on angiogenesis and cytokine levels in rat sponge implants. Br J Pharmacol 1996;118:1584–1591.
19. Freund KB, Klais CM, Eandi CM, et al. Sequenced combined intravitreal triamcinolone and indocyanine green angiography-guided photodynamic therapy for retinal angiomatous proliferation. Arch Ophthalmol 2006;124:487–492.
20. Rouvas AA, Papakostas TD, Vavvas D, et al. Intravitreal ranibizumab, intravitreal ranibizumab with PDT, and intravitreal triamcinolone with PDT for the treatment of retinal angiomatous proliferation: a prospective study. Retina 2009; 29:536–544.
21. Krzystolik MG, Afshari MA, Adamis AP, et al. Prevention of experimental choroidal neovascularization with intravitreal anti-vascular endothelial growth factor antibody fragment. Arch Ophthalmol 2002;120:338–346.
22. Gragoudas ES, Adamis AP, Cunningham ET Jr, Feinsod M, Guyer DR, VEGF Inhibition Study in Ocular Neovascularization Clinical Trial Group. Pegaptanib for neovascular age-related macular degeneration. N Engl J Med 2004;351: 2805–2816.
23. Spaide RF, Laud K, Fine HF, et al. Intravitreal bevacizumab treatment of choroidal neovascularization secondary to age-related macular degeneration. Retina 2006;26:383–390.
24. Rosenfeld PJ, Brown DM, Heier JS, et al, MARINA Study Group. Ranibizumab for neovascular age-related macular degeneration. N Engl J Med 2006;355:1419–1431.
25. Brown DM, Kaiser PK, Michels M, et al. ANCHOR Study Group Ranibizumab versus verteporfin for neovascular age-related macular degeneration. N Engl J Med 2006;355:1432–1444.
26. Dhalla MS, Shah GK, Blinder KJ, Ryan EH Jr, Mittra RA, Tewari A. Combined photodynamic therapy with verteporfin and intravitreal bevacizumab for choroidal neovascularization in age-related macular degeneration. Retina 2006;26:988–993.
27. Ladas ID, Kotsolis AI, Papakostas TD, Rouvas AA, Karagiannis DA, Vergados I. Intravitreal bevacizumab combined with photodynamic therapy for the treatment of occult choroidal neovascularization associated with serous pigment epithelium detachment in age-related macular degeneration. Retina 2007;27:891–896.
28. Kaiser PK, Registry of Visudyne AMD Therapy Writing Committee, Boyer DS, Garcia R, et al. Verteporfin photodynamic therapy combined with intravitreal bevacizumab for neovascular age-related macular degeneration. Ophthalmology 2009;116:747–755.
29. Saito M, Shiragami C, Shiraga F, Nagayama D, Iida T. Combined intravitreal bevacizumab and photodynamic therapy for retinal angiomatous proliferation. Am J Ophthalmol 2008;146:935–941.
30. Treatment of Age-Related Macular Degeneration with Photodynamic Therapy (TAP) Study Group. Photodynamic therapy of subfoveal choroidal neovascularization in age-related macular degeneration with verteporfin: one-year results of 2 randomized clinical trials—TAP Report 1. Arch Ophthalmol 1999;117:1329–1345.
31. Tatar O, Adam A, Shinoda K, et al. Influence of verteporfin photodynamic therapy on inflammation in human choroidal neovascular membranes secondary to age-related macular degeneration. Retina 2007;27:713–723.
32. Tatar O, Adam A, Shinoda K, et al. Expression of VEGF and PEDF in choroidal neovascular membranes following verteporfin photodynamic therapy. Am J Ophthalmol 2006;142: 95–104.
33. Borrillo JL, Sivalingam A, Martidis A, Federman JL. Surgical ablation of retinal angiomatous proliferation. Arch Ophthalmol 2003;121:558–561.
34. Meyerle CB, Freund KB, Iturralde D, et al. Intravitreal bevacizumab (Avastin) for retinal angiomatous proliferation. Retina 2007;27:451–457.
35. Joeres S, Heussen FM, Treziak T, Bopp S, Joussen AM. Bevacizumab (Avastin) treatment in patients with retinal angiomatous proliferation. Graefes Arch Clin Exp Ophthalmol 2007;245:1597–1602.
36. Okamoto N, Tobe T, Hackett SF, et al. Transgenic mice with increased expression of vascular endothelial growth factor in the retina: a new model of intraretinal and subretinal neovascularization. Am J Pathol 1997;151:281–291.
37. Fung AE, Lalwani GA, Rosenfeld PJ, et al. An optical coherence tomography-guided, variable dosing regimen with intravitreal ranibizumab (Lucentis) for neovascular age-related macular degeneration. Am J Ophthalmol 2007;143: 566–583.
38. Kiss CG, Geitzenauer W, Simader C, et al. Evaluation of ranibizumab-induced changes in high-resolution optical coherence tomographic retinal morphology and their impact on visual function. Invest Ophthalmol Vis Sci 2009;50: 2376–2383.
39. Rouvas AA, Papakostas TD, Ladas ID, Vergados I. Enlargement of the hypofluorescent post-photodynamic therapy treatment spot after a combination of photodynamic therapy with an intravitreal injection of bevacizumab for retinal angiomatous proliferation. Graefes Arch Clin Exp Ophthalmol 2008;246:315–318.
40. Spaide RF, Sorenson J, Maranan L. Combined photodynamic therapy with verteporfin and intravitreal triamcinolone acetonide for choroidal neovascularization. Ophthalmology 2003; 110:1517–1525.
41. Bhavsar AR, Ip MS, Glassman AR, DRCRnet and the SCORE Study Groups. The risk of endophthalmitis following intravitreal triamcinolone injection in the DRCRnet and SCORE clinical trials. Am J Ophthalmol 2007;144:454–456.

Molecular Vision 2010; 16:425-437 <http://www.molvis.org/molvis/v16/a48>
Received 28 December 2009 | Accepted 5 March 2010 | Published 12 March 2010

TRPM1 mutations are associated with the complete form of congenital stationary night blindness

Makoto Nakamura,[1] Rikako Sanuki,[2,3] Tetsuhiro R. Yasuma,[1] Akishi Onishi,[2,3] Koji M. Nishiguchi,[1] Chieko Koike,[2,4] Mikiko Kadowaki,[2] Mineo Kondo,[1] Yozo Miyake,[1,5] Takahisa Furukawa[2,3]

[1]Department of Ophthalmology, Nagoya University Graduate School of Medicine, Nagoya, Japan; [2]Department of Developmental Biology, Osaka Bioscience Institute, Osaka, Japan; [3]JST, CREST, Suita, Osaka, Japan; [4]JST, PRESTO, Kawaguchi, Saitama, Japan; [5]Department of Orthoptics and Vision Science, Aichi Shukutoku University, Nagoya, Japan

Purpose: To identify human transient receptor potential cation channel, subfamily M, member 1 (*TRPM1*) gene mutations in patients with congenital stationary night blindness (CSNB).

Methods: We analyzed four different Japanese patients with complete CSNB in whom previous molecular examination revealed no mutation in either nyctalopin (*NYX*) or glutamate receptor, metabotropic 6 (*GRM6*). The ophthalmologic examination included best-corrected visual acuity, refraction, biomicroscopy, ophthalmoscopy, fundus photography, Goldmann kinetic perimetry, color vision tests, and electroretinography (ERG). Exons 2 through 27 and the exon-intron junction regions of human *TRPM1* were sequenced.

Results: Five different mutations in human *TRPM1* were identified. Mutations were present in three unrelated patients with complete CSNB. All three patients were compound heterozygotes. Fundus examination revealed no abnormalities other than myopic changes, and the single bright-flash, mixed rod-cone ERG showed a "negative-type" configuration with a reduced normal a-wave and a significantly reduced b-wave amplitude. Our biochemical and cell biologic analyses suggest that the two identified IVS mutations lead to abnormal TRPM1 protein production, and imply that the two identified missense mutations lead to the mislocalization of the TRPM1 protein in bipolar cells (BCs).

Conclusions: Human *TRPM1* mutations are associated with the complete form of CSNB in Japanese patients, suggesting that TRPM1 plays an essential role in mediating the photoresponse in ON BCs in humans as well as in mice.

The complete form of congenital stationary night blindness (CSNB) is a subtype of Schubert-Bornschein CSNB in which the fundus is essentially normal except for myopic changes [1-5]. From early childhood, patients with complete CSNB lack rod function and experience night blindness. Nystagmus and amblyopia sometimes accompany the other symptoms, and the clinical course is stationary. Best-corrected visual acuity is mildly reduced, and high to moderate myopia is usually found. Electroretinogram (ERG) examinations reveal absent depolarization of neuron by light (ON)-responses (b-wave), and previous extensive physiologic studies indicated that the pathology in complete CSNB lies in the dysfunction of the depolarizing ON bipolar cell (BC). There are two hereditary patterns for complete CSNB: X-linked recessive and autosomal recessive [4].

To date, two genes, the leucine-rich proteoglycan nyctalopin gene (*NYX*)—encoding the glycosylphosphatidylinositol (GPI)-anchored extracellular protein nyctalopin [6,7]—and the *GRM6* gene—encoding the metabotropic glutamate receptor mGluR6—have been identified as the mutated gene in X-linked recessive and autosomal recessive complete CSNB [8-10], respectively. Both nyctalopin and mGluR6 proteins are distributed on the postsynaptic ON BCs and are required for the depolarization of the cell. The *NYX* gene appears to be the major, and possibly only, causative gene for X-linked recessive complete CSNB since *NYX* gene mutations were identified in the majority of X-linked recessive families with complete CSNB. In contrast, *GRM6* gene mutations have been found in only some of the autosomal recessive families with complete CSNB, indicating the existence of other unknown genes for autosomal recessive complete CSNB.

We previously identified a mouse transient receptor potential cation channel, subfamily M, member 1 (*Trpm1*) homolog of human *TRPM1* [11]. *Trpm1* is alternatively spliced, resulting in the production of a long form protein (trpm1-L) and a short N-terminal form devoid of transmembrane segments (trpm1-S). Although mouse trpm1-S was previously identified as melastatin [12], mouse trpm1-L has not been identified. Without distinction between trpm1-L or trpm1-S, trpm1 has been reported to be detected in human primary melanocytes [13], poorly metastatic melanoma cell lines [14,15], mouse retinal pigment epithelium (RPE) [16], and subsets of ON and hyperpolarization of neuron by light (OFF) BCs [17,18]. We found that trpm1-L localization is developmentally restricted to the dendritic tips of ON BCs in

Correspondence to: Takahisa Furukawa, Department of Developmental Biology, Osaka Bioscience Institute, JST, CREST, Suita, Osaka, Japan; Phone: +81668724853; FAX: +81668723933; email: furukawa@obi.or.jp